

CHARACTERIZATION OF THE ADHESIVE INTERFACE BETWEEN RUBBER
AND BRASS PLATED STEEL TIRE CORDS

by
Ashok Sabata

thesis submitted to the Faculty of the
Virginia Polytechnic Institute and State University
in partial fulfillment of the requirements for the degree of
Master of Science
in
Materials Engineering

APPROVED:

W. J. van Ooij, Chairman

Thomas C. Ward

Jack L. Lytton

Characterization of the adhesive interface between rubber
and
brass plated steel tire cords.

by

Ashok Sabata

van Ooij, Chairman

Materials Engineering

(ABSTRACT)

Extensive use of steel belted radial tires made it necessary to investigate the rubber-brass adhesion. Surface analysis techniques were used to give a better understanding of this bond. After about a decade of research, investigators have been successful in optimizing many of the parameters to obtain a bond of high strength. However there are still certain areas in which more work has to be done to make better quality tires. One such area is the effect of compound formulation on adhesion. Compound formulations still to a large extent are empirical. The purpose of this work is to give a scientific basis for formulating the rubber compound for best possible adhesion.

Acknowledgements

The author wishes to acknowledge the support and constant guidance from the committee chairman Dr. van Ooij. The model used in this work was done by Dr. van Ooij.

The author also wishes to acknowledge the constant support of Dr. J.L. Lytton and Dr. T.Ward. With out the help and co-operation of _____, Lab supervisor, this work would not have been completed in time.

The author wishes to acknowledge the help given by his friends in the different stages of the thesis, especially Kannan who helped in the typing of the thesis.

This work was sponsored by Pirelli (in Milan, Italy).

Table of Contents

1.0	INTRODUCTION	1
2.0	LITERATURE REVIEW	3
2.1	Parameters affecting rubber-brass adhesion	3
2.2	Models describing rubber-brass adhesion	4
2.2.1	Haemer's model	5
2.2.2	Van Ooij's model	6
2.3	Effect of compound formulation on adhesion	7
2.3.1	Sulfur to accelerator ratio	8
2.3.2	Accelerators and other compounding ingredients	8
2.3.3	Effect of adhesion promoters	9
2.4	Effect of aging on the interfacial film	10
2.4.1	Heat aging	11
2.4.2	Humidity aging	11
2.5	Summary of van Ooij's model	12
2.6	Scope of work	13
3.0	EXPERIMENTAL WORK	14
3.1	Specimen preparation	14
3.2	Interfacial film preparation	15
3.3	Instrumentation	17
3.3.1	Basic principles	18

3.3.2	SEM	18
3.3.3	EDX	19
3.4	Interface analysis procedure	19
4.0	RESULTS AND DISCUSSIONS	21
4.1	Comparison of different sample preparation methods	21
4.2	Characterization of the interfacial film	23
4.2.1	Effect of aging	23
4.2.2	Composition of the sulfide film along the depth	26
4.2.3	Effect of compound formulation	27
5.0	SUMMARY AND CONCLUSIONS	32
6.0	RECOMMENDATIONS FOR FUTURE WORK	36
	BIBLIOGRAPHY	39

LIST OF FIGURES

Figure 1a.	A) Inside of a radial truck tyre. B) Pirelli radial ply truck tyre.	55
Figure 1b.	A) Nomenclature of the parts of a tubeless truck tyre. B) Construction of brass plated steel tyre cords.	56
Figure 2.	Dimensions of a typical specimen used.	57
Figure 3.	Schematic of interfacial sulfide film in rubber brass bonding showing mechanical interlocking. (Ref. 2).	58
Figure 4.	Schematic of effect of oxygen and water on brass corrosion. (Dezincification) (Ref.2).	59
Figure 5.	Schematic representation of the mechanism of rubber brass adhesion degradation during aging. (Ref. 4).	60
Figure 6.	Schematic illustration of the principal results of the interaction of an electron beam with a specimen.	61
Figure 7.	Components of a typical energy dispersive micro-analysis system.	62
Figure 8.	Comparison of the results of dissolution by nitric acid and potassium per sulfate.	63
Figure 9.	Typical interfacial film in unaged samples at different magnifications (903).	64
Figure 10.	Comparison between zinc rich and copper rich regions in steam aged samples.	65
Figure 11.	Comparison between unaged, humidity aged and steam aged	

	samples.	66
Figure 12a.	Plot of Cu/S and Zn/S ratios of all unaged samples.	67
Figure 12b.	Plot of the adhesion strengths of all unaged samples.	67
Figure 12c.	Plot of S, Cu and Zn contents of all unaged samples.	67
Figure 12d.	Interfacial film composition of all unaged samples.	46
Figure 13a.	Plot of Cu/S and Zn/S ratios of all humidity aged samples.	68
Figure 13b.	Plot of adhesion strengths of all humidity aged samples.	68
Figure 13c.	Plot of S, Cu and Zn contents of all humidity aged samples.	68
Figure 13d.	Interfacial film composition of humidity aged samples.	47
Figure 14a.	Plot of Cu/S and Zn/S ratios at the center and the edge (of the sample).	69
Figure 14b.	Comparison of Cu/S ratio between the center and the edge.	70
Figure 14c.	Comparison of Zn/S ratio between the center and the edge.	70
Figure 14d.	Comparison of sulfur content between the center and the edge.	70
Figure 14e.	Comparison of zinc content between the center and the edge.	70
Figure 14f.	Comparison of copper content between the center and the edge.	70
Figure 15a.	Comparison of Cu/S ratio between humidity aged and unaged samples.	71
Figure 15b.	Comparison of Zn/S ratio between humidity aged and unaged samples.	71
Figure 15c.	Comparison of adhesion strength between humidity aged and unaged samples.	71
Figure 16a.	Plot of Cu/S and Zn/S ratio of the steam aged samples (center region).	72

Figure 16b.	Plot of adhesion strengths of steam aged samples.	72
Figure 16c.	Plot of S, Cu and Zn contents of steam aged samples.	72
Figure 16d.	Interfacial film composition of steam aged samples.	48
Figure 17a.	Comparison of Cu/S ratio between steam aged and unaged samples.	73
Figure 17b.	Comparison of Zn/S ratio between steam aged and unaged samples.	73
Figure 17c.	Comparison of adhesion strengths between steam aged unaged samples.	73
Figure 18a.	Plot of S, Cu and Zn contents in compound 899 in different aging conditions.	74
Figure 18b.	Plot of S, Cu and Zn contents in compound 904 in different aging conditions.	74
Figure 19.	Comparison of depth profiles of compound 899S and 905S.	75
Figure 20a.	Depth profile of all elements in 899S.	76
Figure 20b.	Depth profile of all elements in 900S.	76
Figure 20c.	Depth profile of all elements in 905S.	76
Figure 21a.	Depth profile of all elements in 899H.	77
Figure 21b.	Depth profile of all elements in 904H.	77
Figure 21c.	Depth profile of all elements in 902S.	77
Figure 22.	Plot of silicon contents in steam aged samples.	78

LIST OF TABLES

TABLE I.	Compound formulations of all the samples studied.	40
TABLE II.	Tabulation of adhesion strengths of all the samples.	41
TABLE III.	Summary of sample preparation techniques.	42
TABLE IV.	Sulfide film composition of all the compounds. (at 10kV)	43
TABLE V.	Sulfide film composition of all the compounds. (at 20kV)	44
TABLE VI.	Comparison of the film composition in the different regions of the sample.	45
TABLE VII.	Comparison of silicon content in steam aged compounds.	78
TABLE VIII.	Comparison of the film composition in unaged aged samples with different compound formulations.	46
TABLE IX.	Comparison of the film composition in humidity aged samples with different.	47
TABLE X.	Comparison of the film composition at center of all the steam aged samples.	48
TABLE XI.	Comparison of the film composition at the edge of all the steam aged samples.	49
TABLE XII.	Comparison of film composition between humidity and unaged samples.	50
TABLE XIII.	Comparison of film composition between steam aged and unaged samples.(at the center)	51
TABLE XIV.	Comparison of film composition between steam aged and unaged samples.(at edge)	52

TABLE XV.	Comparison of film composition between the edge and center of the samples.	53
TABLE XVI.	Comparison of compounds 899 and 904.	54

ABBREVIATIONS

- AES : Auger Electron Spectroscopy.
- CBS : N-cyclohexyl-2-benzothiazole sulfenamide.
- DCBS : N,N-dicyclohexyl-2-benzothiazole sulfenamide.
- EDX : Energy Dispersive X-ray Analysis.
- OBTS : N, N-oxidiethylenebenzothiazole sulfenamide.
- SEM : Scanning Electron Microscope.
- STEM : Scanning Transmission Electron Microscope.
- XPS : X-ray Photoelectron Spectroscopy.

1.0 INTRODUCTION

In automotive tires, steel cords have been used as reinforcing material for quite some time. These cords are of complicated construction as shown in Figure 1. During vulcanization a bond is formed between the natural rubber of the tire cord skim stock and the steel wires. The performance of tires is, to a large extent, dependent on the strength and the durability of this bond. In order to enhance the bonding of steel to rubber some sort of adhesive is used. One of the major adhesives used in the tire industry is the brass plated tire cords. The cords are plated with 200nm brass which bonds the cords to the rubber of the tyre during its vulcanization.

The adhesion mechanism of this steel cord to rubber is quite unique in adhesion science. Adhesion builds up as a result of a surface reaction on the brass coating during rubber vulcanization. The copper and zinc of the brass react with the sulfur of the rubber compound and form an interfacial layer. This interfacial layer consists of a mixture of sulfides and oxides of both copper and zinc. This layer may reach a thickness of a few hundred angstroms and can be considered as the adhesive formed in situ. However the nature of the bonding (i.e. chemical bonding or mechanical interlocking) of this sulfide layer is still a matter of dispute.

The chemical, mechanical, adhesive and corrosion inhibiting properties of the sulfide film is dependent on mainly two parameters. They are :-

1. Cord parameters like the brass copper content, its thickness etc.
2. Compound formulation of the rubber.

Cord parameters have been studied in detail and more or less have been optimized. Optimum brass composition and brass thickness have been reported by researchers in the literature. In actual tire practice the levels of the compounding ingredients are determined in an empirical way. To provide a scientific basis for the observed adhesion characteristics a more detailed study of the relationship between the properties of the sulfide film and the compound formulations is required.

PIRELLI (in Milan, Italy) is interested in improving the bonding quality of their tires. Hence this project, which is sponsored by them, is being carried. The aim of this project is to study the relationship between the composition, structure and the environmental degradation of the interfacial film with natural rubber compounds of known formulation. Due to the high bonding forces involved at the interface it has been difficult to reach the interfacial layer and conduct an analytical study. In this work different experiments have been performed to get access to the interfacial film and characterize it. Papers written by researchers have been reviewed in an effort to understand the adhesion between brass and rubber. The contents of these are included in the literature survey which follows.

2.0 LITERATURE REVIEW

There is an abundant supply of literature on the various aspects of rubber-brass adhesion. The availability and industrial usefulness of surface and thin film analysis techniques had led to a series of fundamental studies on the steel cord to rubber-brass adhesion mechanism. Van Ooij and Haemer have published excellent reviews and state of the art articles on this subject (1,2,3).

To explain the type of bonding mechanism between the rubber and the brass, different models have been proposed by many research workers. Although the actual type of bond between the interfacially formed copper sulfide film and the cured network still has not been identified conclusively, this aspect of rubber-brass adhesion is becoming rather irrelevant since the literature is unanimous that bond failure seldom occurs between the copper sulfide and rubber, but usually cohesively within the sulfide film or adhesively at the interface sulfide and the brass substrate.

2.1 Parameters effecting rubber-brass adhesion

The parameters that effect the rubber brass adhesion, are those which effect the composition and the thickness of the interfacial film. These are the cord parameters and the rubber compound formulation. The cord parameters are:-

1. Copper content and the thickness of the brass layer.
2. Zinc oxide content of the brass surface. (This acts as a passivating agent).
3. Also important is the presence of inhibitors on the brass surface.

Researchers have reported that a copper content of around 65% copper gives good adhesion. Brass with higher copper content give a thick interfacial layer which has mainly Copper sulfide. This is because of the p-type semiconductor nature of the sulfide film. This allows metal ions to diffuse rapidly and form new sulfides. The thick sulfide layer formed is very sensitive to brittle fracture resulting in low pull out forces. The low copper content brass forms excessive zinc sulfide which being a n-type semiconductor, blocks the diffusion of metal ions so that a further growth of the reaction layer through metallic diffusion is prevented. As it is copper sulfide which is required for good adhesion, not zinc sulfide, the adhesion strength is low.

Optimum cord parameters have been described later in the models. Also, the compounding parameters have been dealt later as a separate section.

2.2 Models describing rubber-brass adhesion

There are basically two different models which have been used in the literature to explain the rubber-brass adhesion. These models will be described briefly in this section.

2.2.1 Haemer's Model

Haemer has proposed that the bonding is chemical in nature. According to him the actual bonding mechanism is the penetration of the $NR - S_y$ (pendant groups) into the sulfide film which results in $Cu_xS - S_y - NR$. The characteristic feature of Haemer's model is the concept of synchronization. Optimum adhesion is dependent on the synchronization of the rate of sulfidation of brass and the rubber cure. If the reaction is either too fast or too slow the adhesion begins to drop.

This model has been able to explain many of the experimental results. The dependence of adhesion on the copper content of the brass can be explained by the formation of ZnS at low copper content. This ZnS forms underneath the copper sulfide and it acts as a barrier layer for copper diffusion. Cobalt is used as an adhesion promoter and its effect is explained using the synchronization principle. Cobalt effects the copper sulfide defect structure which leads to the slowing down of the rate of copper sulfide formation. It also accelerates the cure of the compound. There are certain setbacks in Haemer's model. It cannot explain the large differences between optimum cobalt contents in compounds for brass and for zinc bonding. As Haemer's model proposes that there is chemical bonding of copper sulfide to rubber then a monolayer of this sulfide should be sufficient to ensure good adhesion. But in literature a minimum critical copper sulfide thickness has been reported. Also, this model cannot explain the fact that there is adhesion even without cobalt or with insoluble cobalt salts.

2.2.2 Van Ooij's Model

This model assumes the bonding to be physical in nature. According to this model the copper sulfide dendrites, with a high specific area, grow into the compound before the liquid polymer changes into a crosslinked elastomeric network. This gives a tight interlocking of the polymer and the sulfide film. This locking of the polymer molecules into the copper sulfide film is consistent with the observation from diffraction techniques which indicated the presence of crystalline copper sulfide. Whereas according to Haemer's model linking of copper sulfide molecules to the polymer by $Cu_xS - S_y - NR$ would not be consistent with a crystalline copper sulfide lattice.

In Figure 3 a schematic of the bonding of the interface film has been shown. An important criteria for the formation of a good bond is the formation of copper sulfide, its cohesive strength and adhesion to the substrate. Also important are the rate of secondary corrosion reactions which proceed underneath the copper sulfide film once it has formed. In this model ZnS and FeS are not bonding as they do not grow rapidly enough under rubber vulcanization conditions. Also these do not contribute to adhesion because they grow as dense, homogeneous film which donot interlock with the polymers.

For good bond strength and bond durability the cord parameters predicted by this model is a thin brass coating with a high concentration of diffused ions, a low copper content (60-65%) and a thin but very homogeneous ZnO surface layer, which is passivating and contains copper atoms. The presence of homogeneous ZnO layer improves the cord corrosion resistance and the copper atoms help in rapid initial copper sulfide formation and prevention of formation of nonbonding zinc sulfide.

To explain the effect of aging and adhesion degradation, corrosion principles were used in this model which will be described now.

Dezincification effect : The chemical reactions which lead to the development of the rubber brass bond during the vulcanization of the tire, continues to proceed during the service life of the tire. In this process the copper sulfide grow till all the included copper in the zinc has reacted. The formation of thick films leads to the development of strains resulting in cracks and hence reduction in adhesion. After the termination of the copper sulfide film growth zinc ions diffuse to the surface and form either ZnS or $ZnO/Zn(OH)_2$ depending on the moisture content. This removal of Zn from the brass is called dezincification.

If during cure a high amount of moisture is present then a side reaction takes place as shown in Figure 4 . If a poor copper sulfide film has been formed then the zinc ions diffuse through and tend to react with hydroxyl ions generated by the cathodic corrosion reaction. The incorporation of this $ZnO/Zn(OH)_2$ in the film leads to the formation of a weak boundary layer and hence poor adhesion. In order to have a bond of high strength the above mentioned reactions have to be arrested. This has been successfully done by incorporating cobalt or nickel ions into the ZnO layer which reduces its conductivity and prevents diffusion of zinc ions.

2.3 Effect of compound formulation on adhesion

Compound studies have always been carried out, but are still to large extent empirical. This is probably due to the complexity of the system dealt with. Differences between good and poor compounds were found to reside in the composition of the copper sulfide film and its adhesion to the substrate. Studies have

been performed to see the effect of the sulfur to accelerator ratio, type of accelerator, adhesion promoters etc. These will now be discussed in detail.

2.3.1 Sulfur to Accelerator Ratio

The major compound parameter that has an effect on adhesion to brass is the sulfur-to-accelerator ratio. The brass is sulfidized by intermediates of the type $R - S - S_y - NR$, where R is an accelerator fragment, rather than by free sulfur. The properties of the copper sulfide film, such as adhesion, cohesion and stability in corrosive environments depend on the type of copper sulfide formed. In general high sulfur-to-accelerator ratios i.e. greater than 4 form stable copper sulfide films which lead to high adhesion. High values of y in the intermediate lead to good copper sulfide films, whereas low values produce poor films, regardless of the quality of the cord. It has been reported that the best compounds are those which have high sulfur levels and high sulfur-to-accelerator ratios (2).

2.3.2 Accelerators and other compounding ingredients

Normally for bonding brass plated steel cords sulfenamide type accelerators are most commonly used. Some of the different types of accelerators are MBT, MBTS, CBS, TBBS, DCBS, MBS etc. Some authors have done a comparative study on the different types of accelerators and concluded that sulfenamides like CBS, TBBS, DCBS, MBS give high bond strengths. One probable reason given was that the sulfenamides had relatively slow reaction rates. It is also reported that the DCBS is better than other

sulfenamide accelerators. The explanation given was that, during the induction period the DCBS molecules are still undecomposed and they are adsorbed on the brass surface to a lesser extent than other sulfenamides (probably due to steric effect). Hence inhibition of brass corrosion by sulfur is less in case with DCBS.

The type of accelerator is also important in aging tests as it determines the sensitivity of the bond to moisture. Here too DCBS was found to be a favourable choice. It has been reported that higher accelerator levels increase the moisture sensitivity of the bond.

The effect of other compound ingredients is not much on the adhesion. Carbon black's effect is predominantly of mechanical nature, it reinforces the polymer and hence a high pull out force is normally required. Stearic acid does not have an effect on adhesion, as it is very corrosive to brass. However it attacks the ZnO film and dissolves it. Hence the zinc oxide used in the compound is important here. The ZnO in the compound should be very reactive to stearic acid, and the ratio of zinc oxide to stearic acid should be sufficiently high.

2.3.3 Effect of adhesion promoters

Cobalt and nickel salt have been used as adhesion promoters for quite some time. Some common cobalt salts are cobalt naphthenate, cobalt stearate, Manobond C (this is a complex mixture of various cobalt salts of C_9 , C_{10} and C_{11} aliphatic acids and also some cobalt oxyborates). Metal organic cobalt salts, which are soluble in the compound have two effects (4).

1. They accelerate the cure and increase the crosslink density for high sulfur stocks.

2. Due to the presence of cobalt salts there is a displacement reaction at the brass surface and formation of inorganic cobalt ions at the interface during the cure.

Cobalt improves initial and aged adhesion. Initial adhesion is improved because of the increase in the crosslink density in its presence. The aged adhesion is improved due to its effect on the ZnO layer. If sufficient amount of cobalt ions are incorporated into the ZnO before sulfidation starts then the formation of zinc ions under the ZnO layer and the migration of these ions to the surface is retarded. There is no effect on the copper ion migration as they migrate along the grain boundaries of the ZnO layer. Hence with the use of cobalt salts the initial formation of ZnS is suppressed and the rapid formation of copper sulfide is stimulated.

The cobalt ions in the ZnO film also reduces its conductivity, this is beneficial to the sensitivity of brass to dezincification effects, during postcure aging. Hence, steam aged adhesion will be improved. However a small and very critical amount of soluble cobalt salts must be used for steam aged protection.

2.4 Effect of aging on the interfacial film

The tires have long service life and they are also submitted to severe environmental conditions. Hence studies have been carried out on maintaining adhesion under different testing conditions. The parameters involved in tire aging simulation testing are temperature, time, humidity and the presence of aggressive media.

2.4.1 Heat Aging

In heat aging conditions the rubber compound is effected and partially the adhesion loss could be attributed to rubber degradation (5). The brass thickness and its copper content also have effect on the heat aging results. It has been shown that the adhesion loss is low with brass having 65-70% copper. Also there is an increase in the zinc sulfide content in the reaction layer. Because of its high resistivity the increase in zinc sulfide is beneficial to corrosion protection. This prevents small local corrosion currents to flow through the interface. However there should be enough copper sulfide for bonding purposes.

With long heat aging times there is a change in the stoichiometry of the copper sulfide from Cu_xS towards Cu_2S (6). This leads to an adhesion loss as Cu_2S is nonbonding because of its inability to form donor-acceptor bonds.

2.4.2 Humidity Aging

Different humidity tests have been performed and all show the detrimental effect of water on adhesion (7). In cured humidity aging and in steam aging tests there is a high consumption of the brass layer. This leads to an increase in the thickness of the film, giving rise to risk of brittle fractures.

The compound formulations have a greater effect on the adhesion as compared to the brass composition. There is formation of zinc sulfide in combination with zinc oxide in these aging conditions. This ZnS/ZnO layer forms a weak boundary layer which leads to adhesion losses.

In a steam aging test the film is attacked by water. As explained earlier, a simple corrosion cell is formed leading to the generation of zinc ions and the incorporation of zinc hydroxide in the ZnO layer. Then zinc ions diffuse to the surface where it dissolves and reprecipitates as zinc hydroxide. These are all part of the complex set of reactions called 'dezincification'. The zinc hydroxide destroys the integrity of the copper sulfide film and hence, adhesion.

2.5 Summary of Van Ooij's Model

In this investigation van Ooij's model has been used extensively, hence it will be summarized here. Figure 5 schematically summarizes the reactions at the rubber-brass interface during vulcanization and during postvulcanization aging. A sulfide film is formed during the initial stages of the rubber cure by reaction between active sulfur containing intermediates and copper atoms contained in the ZnO film at the brass surface. The bonding mechanism is a tight interlocking of crosslinked polymer in the porous copper sulfide film. Though ZnS is formed it does not adhere as it is not porous. The presence of cobalt in the compound reduces the conductivity of the semiconducting film. This results in the suppression of ZnS formation and stimulation of copper sulfide formation.

A complex series of solid state and surface reaction proceeds during the postvulcanization aging of the rubber-brass bond. The formation of zinc ions at the metal-film boundary (anodic reaction product) is the rate determining step. Due to the diffusion of these ions and electrons to the surface, an overgrowth of copper sulfide by ZnS and zinc hydroxide takes place. This step is then followed by dissolution of zinc hydroxide. In the above reactions the conductivity of copper sulfide and ZnO films are

important. Adhesion promoters such as cobalt reduce the conductivity of the ZnO film and hence improve the resistance to adhesion degradation effects induced by dezincification. The conductivity of the copper sulfide film depends on its composition and structure which are a function of the formulation of the compound. High sulfur-to-accelerator levels give films with low conductivity and good thermal and chemical stability. Poor films are formed when the sulfur-to-accelerator ratio drops below 4.

2.6 Scope of Work

The review of the literature shows that rubber brass adhesion has been studied in detail for the past decade. Also surface sensitive methods like XPS, AES, SIMS, SEM etc have been used extensively to study the adhesion mechanism. However no detailed study on relationship between sulfide layer and compound formulation has been done, probably because of extreme sample preparation difficulties. The objectives of this project are :

1. To get access to the interfacial film through different experimental techniques.
2. To see the effect of the change in rubber compound formulations on the rubber-brass adhesion in different aging conditions (i.e. to characterize the interfacial film.)

3.0 EXPERIMENTAL WORK

Researchers have extensively used surface analysis techniques like ESCA, AES and SIMS to study the copper sulfide film. In this work an electron microscope, with SEM and EDX facility, was used to study the interface. In order to increase the understanding of the mechanism of the rubber-brass interface and to be able to explain and predict different adhesion behaviours, it is necessary to examine the morphological, compositional, crystallographic and mechanical properties of these sulfidic reaction layers. However because of the high bonding forces involved and, the presence of the rubber and the brass, make it fairly difficult to reach the interface layer and conduct an analytical study. Therefore a lot of time and effort was spent on the sample preparation technique to get access to the sulfide film. In this chapter, the materials used, specimen preparation, instrumentation used and the procedure followed in the present investigation are described.

3.1 Specimen Preparation

The specimen used in this investigation had the dimensions as shown in Figure 2. The substrates were cold worked brass of 65.7% copper. Before bonding, the metal strips were cleaned with a fine abrasive powder (wet) or with a fine grade

sand paper (wet). The cleaned specimen were then stored in a desiccator over a desiccant.

In this investigation, to characterize the interfacial film seven compound formulations were studied. The base compound is denoted by "C" and is given the sample number 899. The modifications made with this compound are shown in Table I. These modifications were made such that the effect of different compounding parameters could be studied. DCBS and OBTS are the two accelerators which were examined in this investigation. Manobond 680C is an cobalt adhesion promoter. This is present in compound 904 and 905. The other variations made were in relation to the S/Accelerator levels. The brass strips were adhered to the rubber by vulcanizing in a heated press for 40 minutes at 150 degree C. The final thickness of the cured rubber was about 0.5 mm.

Besides preparing samples in the standard cure conditions some samples were prepared in humidity aged and steam aged conditions. The humidity aged samples were aged in a humidity cabinet at 55 degree C and 90 % relative humidity for 11 days (some samples were prepared with time durations of 7 days and 14 days, but these have not been studied in this work). The steam aged specimens were aged in saturated steam at 120 degree C for 24 hours. The adhesion testing of all the specimens prepared was done using standard Pirelli procedures and the values obtained in these tests are shown in Table II.

3.2 Interfacial Film Preparation

Four different techniques were used to get access to the interfacial film.

1. Liquid Nitrogen Technique.
2. Dissolution of Brass in Nitric Acid.
3. Dissolution of Brass in a solution of Iodine + Methanol.
4. Dissolution of Brass in Acidified potassium per sulfate.

Table III shows the performance of each of these methods. In the liquid nitrogen technique the cured samples were immersed in liquid nitrogen and then pulled apart quickly. Under these conditions normally one would get an adhesion failure due to the stiffening of the rubber. However in our samples the failure appeared to be more or less in the rubber. No sulfide layer was observed on the rubber surfaces. This was confirmed by using SEM, EDX and ESCA analysis.

The other three techniques to get access to the sulfide film, involved the dissolution of the brass. This dissolution was done using different oxidizing agents. However one should be careful about the effect of these oxidizing agents on the interface layer. Before the dissolution the specimens were thinned, i.e. the brass plates, mechanically on a grinding wheel. Acids like sulfuric acid, nitric acid etc are some of the commonly used oxidizing agents. Dilute Nitric acid was used to chemically thin the brass plates. This was followed by the final thinning which involved the total removal of the brass in an electrolytic manner. During the whole experiment the dissolution could be observed from the change in the color of the solution to light blue. Though the experiment was successful in dissolving the brass, EDX and SEM analysis showed regions where the copper sulfide film was effected.

As the copper sulfide is very conducting it is quite possible that electrolytic dissolution may have an effect on the film. Hence, modifications were made in the experiment. The acid was made more dilute i.e. 5ml of conc. nitric acid in 20ml of water, and the final thinning step was not used. This was partially successful. It was

also observed that as the concentration and time of exposure of the copper sulfide film to acid increased, there was more risk of it getting affected by the acid.

Iodine in methanol solution has been successfully used in dissolving steel (8). This method was used in an attempt to dissolve the brass. Oxygen free methanol was saturated with Iodine and then nitrogen was bubbled to keep it oxygen free. After the initial mechanical thinning the sample was introduced in the solution and kept for 5-6 hours. The sample was then rinsed in pure dry methanol for 24 hours in order to remove the iodide and the excess iodine. Unfortunately, EDX analysis showed the presence of large amounts of iodine on the rubber which was not possible to remove.

The dissolution of the brass in acidified potassium per sulfate was by far the most successful method used in getting access to the sulfide film. About 2gm of potassium per sulfate was dissolved in 20ml of water and then 1ml of conc. nitric acid was added to acidify it. The mechanically thinned specimen was introduced in to this solution for 3 hours. It was observed that in this time the brass separated from the rubber with the copper sulfide film on the rubber.

3.3 Instrumentation

In order to study the interfacial film different instruments like the SEM, EDX etc. were used. In this project a Philips 420 STEM and a Tracor Northern EDX system was used. In this section a brief description of the basic principles of these instruments will be given.

3.3.1 Basic Principles

In an electron column, electrons are accelerated through an electric field, thus acquiring kinetic energy. This energy is deposited in the sample and its dissipation yields a variety of signals for analysis as depicted schematically in Figure 6. As suggested by the figure, Auger and secondary electrons emerge from near the sample, surface and elastically scattered electrons are typically scattered through larger angles than are inelastically scattered electrons. Secondary electrons escape from the sample to be detected only if they are created near the surface. This gives them sensitivity towards the topography of the sample and is used in the SEM. X-rays travel much greater distances through the sample than electrons and therefore escape from depths at which the primary electron beam has been widely spread. The characteristic X-rays indicates the elements from which it came and hence is used for element identification in the EDX.

3.3.2 Scanning Electron Microscope

In the SEM a fine electron probe (7-10nm diameter) is used to illuminate the specimen. By scanning the probe across the specimen, and detecting the low energy secondary or high energy primary back scattered electrons returning from the surface, an image is formed. This returning electron signal is fed into a cathode ray tube (CRT) scanning at the same rate, and a time dependent image is thus obtained. Surface topography and/or elemental changes give rise to different signal intensities and hence contrast is obtained on the CRT. The Philips 420 STEM (scanning mode) was used for SEM work. Also, a JEOL 840 SEM was used for studying large samples.

3.3.3 Energy Dispersive X-ray Analysis

The components of a typical energy dispersive microanalysis system is shown schematically in Figure 7. It is the array of components from detector to multichannel analyzer that assembles the information contained in the x-ray signals into a convenient x-ray spectrum.

All EDX spectrometers have in common a solid state detector. For microanalysis, this detector is almost always manufactured from a single crystal of silicon. The signal processing is done in a series of steps by a preamplifier, pulse processor and a multichannel analyser. The details of x-ray instrumentation have been reported in the literature (9). In this work a Tracor Northern EDX system was used for most of the analysis, part of the analysis was also done on a Kevex system.

3.4 Interface Analysis Procedure

As rubber is nonconducting it is necessary to coat the sample with carbon for SEM imaging. However when there is a good copper sulfide film this was not necessary because copper sulfide is a good conductor. After mounting the samples on the SEM sample holder, SEM images were obtained on the CRT at 20KV. Photographs of the sulfide crystals were taken at different magnifications and the EDX spectrums of the corresponding regions were acquired.

In order to get a good x-ray signal (i.e. good count rates) on the EDX detector, the sample holder was tilted towards the detector. EDX spectrums were also collected at 10, 40, 60 and 80KV for a crude depth profile. All the spectrums acquired

were stored in a diskett for further analysis. Using the software for quantitative analysis a compositional analysis of the film was done.

The EDX and SEM analysis was done for the unaged, humidity aged and steam aged samples. During the adhesion testing of the humidity aged samples it was observed that the samples broke cohesively at the edge and adhesively at the center. Also similarly in steam aged samples a difference in color was observed in the center of the samples. Hence SEM and EDX analysis were performed both at the center and edge for humidity and steam aged samples.

4.0 RESULTS AND DISCUSSION

In this chapter the results obtained from the different experiments that were performed have been reported. Also, these results have been discussed and an attempt has been made to explain them using the models discussed in the literature. The results can be broadly classified as of two types:

1. Techniques of getting access to the interfacial film.
2. Characterization of the interfacial film.

The characterization done here is very qualitative in nature. Also presently another graduate student is continuing this project and his work primarily concerns the characterization of the film.

4.1 Comparison of Different Sample Preparation Methods

As explained in chapter 3, different sample preparation techniques had been tried out in order to get access to the interfacial film. SEM and EDX analysis were performed to compare the results of all the techniques. Of all the methods the

potassium per sulfate technique was found to be the most successful one. In Figure 8 a comparison is made between the results of dissolution of brass by acidified potassium per sulfate and by dil. Nitric acid. In the micrograph the amount of copper sulfate crystals seen after the dilute Nitric acid treatment, clearly shows that dil. Nitric acid effects the copper sulfide crystals, and to a large extent dissolves them and exposes the rubber region. Whereas the dissolution by acidified potassium per sulfate didnot effect the sulfide film. A continous layer of copper sulfide is seen in the micrograph.

In order to do a good characterization of the sulfide film it is important to study the microstructure of the interfacial film in the TEM. Different methods to prepare the sample for observation under the TEM were attempted. One of the methods used was to remove the copper sulfide film, using extraction replica technique. Cellulose acrylate was the adhesive used for the extraction of the film. TEM examination showed that the adhesive was not able to remove the copper sulfate film from the rubber. Normally the point of failure of the rubber-brass bond is between the film and the substrate, and never between the film and rubber. This explains the difficulty encountered in removing the film from the rubber.

Another method attempted was to cut thin sections off the rubber using a cryogenic microtome and then the microstructure of the copper sulfide film was observed. This method was also unsuccessful because the sulfide film is very thin and mounting of the sample in the proper orientation and then cutting good sections was difficult. However, this method was used to see the microstructure of the rubber. Rubber samples of pyramid shape were mounted on a sample holder whose diameter was 3mm. Thin sections were cut below the glass transition temperature of the rubber. Liquid nitrogen was used as the cooling agent and the cut sections are normally between 1000 to 2000 Angstroms thick. The microstructures were then observed using a Philips 420

STEM. The microstructures of unaged and steam aged samples were then compared. These showed no change after aging of the samples. From this a conclusion can be made, the change in the adhesion characteristics after aging is solely due to the properties of the interfacial film.

4.2 Characterization of the Interfacial Film

It is important to characterize the interfacial film because the failure of the rubber-brass bond is between the sulfide film and the substrate. The results of all the analysis performed in this investigation have been reported in the form of graphs and tables. The following characteristics have been studied in this investigation :

1. Composition of the sulfide film in relation to the change in the compound formulation.
2. Effect of aging on sulfide film composition.
3. Thickness of the film.
4. Change in the film composition with the time of aging.

All these factors are related to each other, so besides discussing them separately an overall discussion will also be given.

4.2.1 Effect of Aging

Aging tests were carried out to discriminate between the effect of different compound formulations on the interfacial film. Two types of aging tests were performed, viz, humidity aging and steam aging. The composition of the film in the humidity aging

and steam aging conditions have been compared, with that of the corresponding unaged samples, in Tables XII and XIII. Figures 15 and 17 also show these comparisons.

After humidity aging of the unaged samples, an increase in the adhesion strength of all compounds, except compound 899H, is observed. The following trends are observed in figure 15 :-

1. A small increase in the Zn/S ratio in all the compounds.
2. Change in the Cu/S ratio after humidity aging (here too compound 899H was found to be the exception).

One plausible explanation for the increase in the adhesion could be that, during humidity aging there is a recrystallization of the sulfide film resulting in a film which has better properties. Simultaneously there could also be a growth of the sulfide film as indicated by the change in the film composition.

On physical examination of humidity aged samples, a ring was observed between the center and the edge of the sample. The area of this ring changed as the time of aging was increased from 7 days to 14 days. In the adhesion testing experiment, i.e. separating the brass from the rubber using mechanical force at room temperature, the failure in the ring was found to be always adhesive in nature. The comparison of the composition of the film at the center and the edge revealed that there is not much change in the film composition. However, a comparison of the film in the ring with the region outside the ring may be fruitful.

In the steam aging test the film is attacked by water. The reactions that take place are very complex, but the final result is the degradation of the film and the loss of adhesion. The adhesion strength of all the compounds studied were lowered

after steam aging. In some cases the loss was very drastic and in others it was less. Figure 17 compares the composition of the interfacial film between unaged and steam aged samples. The conclusions of this figure are :

1. In all the compounds an increase in the zinc content is seen after steam aging.
2. The Zn/S ratio is hence invariably high in all the steam aged samples.

This is in perfect agreement with the dezincification theory explained in the literature review. The zinc ions diffuse to the surface and form ZnO/zinc hydroxide on the interface, this destroys the copper sulfide film and, therefore the adhesion.

Another observation made was that the composition of the film in the steam aged samples were not uniform. There was a variation in the composition from the edge to the center. These variations have been summarized in Figure 14, and the following conclusions can be drawn:

1. A higher Zn content, thus Zn/S ratio was found in the center.
2. The Cu/S ratio was found to be higher in the edge.

These results indicate the effect of the time of exposure of the interfacial film to the steam. The difference in the composition between the edge and the center can be explained as to be due to the attack of the film by steam, first at the edge and then the center. In other words the edge is exposed to steam for a longer duration of time as compared to the center.

A comparison of the topography of the sulfide film from the center and edge of the sample was done by SEM. This is shown in Figure 10. It was observed that the zinc rich regions (i.e. center) normally had rough features, while the copper rich regions were comparatively very smooth.

4.2.2 Composition of the Sulfide Film along the depth

The depth of penetration of the electron beam has been taken as a measure to gauge the thickness of the film. The composition of the film was found at 10, 20, 40, 60, and 80KV. Figure 20 and 21 give these compositions. These give a qualitative idea of the thickness of the sulfide film. Also interesting is that it gives a crude depth profile of the elements.

There does not seem to be any clear difference in the thickness of the film formed by the different compounds. The thickness seems to lie between 20KV and 40KV for most of the compounds. This is evident from the change in the Cu and Zn concentrations. Compounds 899S, 900S, 902S and 904H have their maximum copper concentrations at 20KV and then it falls down. Similarly in 899H there is a sudden rise in the zinc concentration above 20KV. However, it is difficult to estimate the thickness of 905S as the drop in the copper concentration is gradual.

In compounds 899S, 900S, and 902S the top layer of the interfacial film has very high zinc concentration and low copper and sulfur concentration. As we go along the depth the copper content increases and the zinc content falls and finally levels off to a constant value. The low contents of copper and sulfur at 10KV indicates very little sulfide concentration in the top layer of the interfacial film. The high zinc content confirms the theory that, there is probably a large quantity of a mixture of ZnO/ zinc hydroxide at the surface.

Below this layer there is an increase in Cu and S content, indicating that the initially formed sulfide film has been overgrown by zinc hydroxide after aging.

Higher beam voltages penetrate into the rubber and therefore we see the levelling of all the values. All the depth profile plots were made for the center region of the samples. Data was not available to make similar plots for the other compounds. However a plot could be made for 899S in the edge region. This showed a higher copper content in the top layer, as compared to the center of the sample. The zinc hydroxide layer here is probably much thinner than at the center.

Compounds 904S 905S and 899H have a very high copper content near the top of the interfacial layer. The zinc content was less throughout the interfacial film indicating the absence of ZnO/ zinc hydroxide on the interface. In sample 899H the increase in the zinc content above 20KV is due to the zinc content of the rubber.

In order to get a clearer picture of the thickness of the films additional analysis at other accelerating voltages may help. Also the use of thin film software program in the EDX system (if available) would be very helpful for accurate analysis.

4.2.3 Effect of Compound Formulation

Seven different compound formulations have been studied. The factors that have been considered in studying these formulations are :

1. Sulfur to Accelerator ratio
2. Type of Accelerator used
3. Effect of Adhesion Promoters
4. Effect of Resin systems

The composition of the sulfide film formed in all the samples are summarized in Table IV and V. Comparison of the film composition of the unaged samples is done in Figure 12. The following trends can be seen in the figure:-

1. With increasing copper content there is a decrease in the zinc and the sulfur content.
2. Good correlation between the Cu/S ratio and the adhesion strength.

One of the criteria to evaluate the quality of the sulfide film is to compare the copper to sulfur ratio(2). Poor films generally have high Cu/S ratio and adhere poorly to the substrate. A high Cu/S ratio means that the lattice spacing is higher and, hence poor films have coarser crystallites as compared to the good films.

A high Cu/S ratio compound has low strength. The base compound, i.e. compound 899 has a resorcinol based resin system and the unaged adhesion strength is good. This could be partly explained by the fact that this type of system normally increases the rubber cure and effectuates a higher crosslink density giving a high modulus and hence higher pull out forces. Also, this system is a weak inhibitor for brass corrosion by sulfur. So compound 899 probably forms a good interfacial film (i.e. low Cu/S ratio) in the unaged condition.

Compounds 904 and 905 also have good unaged adhesion. Both these compounds contain cobalt and a resin system, both of which are known to accelerate the cure and increase the crosslink density giving higher pull out forces. Compound 904 also forms an interfacial film with low Cu/S ratio.

Sulfur to accelerator ratio is another important parameter in deciding the adhesion strength. Compounds 903 and 901 have higher sulfur to accelerator ratios and also higher adhesion strength as compared to compound 902. The type of

accelerator used is also important in deciding the initial adhesion strength. Compound 901 uses DCBS as the accelerator while compounds 902 and 903 use OBTS as the accelerator. The unaged adhesion strength of 901 is found to be greater than in 902 and 903. Compound 901 has an interfacial film with lower Cu/S ratio as compared to that formed by compounds 902 and 903. This probably suggests that DCBS forms a better interfacial film as compared to OBTS. Figure 9 shows a SEM micrograph of a typical sulfide film found in the unaged sample. No distinguishing difference was observed between the topographical features of the different unaged sulfide films.

Humidity aging increases the adhesion strength of all the compounds. Table IX summarizes the change in the sulfide film composition with different compound formulations. Here the relation between Cu/S ratio and the adhesion strength is different from that of the unaged samples. In compounds 902H, 903H, 904H, and 905H the trend in the Cu/S ratio can be related to the adhesion strength. Here too a high copper to sulfur ratio means low strength, as was the case for unaged samples.

Compound 899H has a poor adhesion strength. This could be partly because of the resin system in the compound. This resin system has an amine which may get hydrolyzed and thus increase the sensitivity of the film to moisture drastically. In this compound there is no change in the Cu/S ratio after aging, but a small increase in Zn/S ratio is observed. Compound 901H has a very high strength in humidity aging condition. Also, a large increase in Cu/S ratio is observed here. 901H has a higher sulfur-to-accelerator ratio than 899H. In the humidity aged samples also, the effect of sulfur-to-accelerator ratio and the type of accelerator used, is similar to as in the unaged samples.

All the above discussions indicate that in humidity aging the reactions, that have taken place, were helpful in improving the quality of the interfacial film in all compounds except 899H.

The attack of steam on the interfacial film is much more severe than in other aging tests. Table X and XI summarize the effect of steam aging on the interfacial film formed using different compound formulations. Compound 899S, 902S and 903S have poor steam aged strength. There is no way of discriminating between these three, all of them had very high Zn/S ratio and low Cu/S ratio. The depth profiles also indicated a film of ZnO/ zinc hydroxide on the sulfide film which is responsible for the loss of adhesion. Compound 900S has better steam aged adhesion than most other compounds (except compound 904S). 900S has one major difference in its compound formulation as compared to other compounds, i.e., it didnot have any resin system. The depth profile shows a sharp increase in the copper content at 20KV, and also the copper content at the edge is very high. All these probably point to the fact that the ZnO/zinc hydroxide layer in 900S is very thin as compared to the other compounds. The absence of resin system may be one of the causes for the formation of copper sulfide film with a low conductivity and hence leading to a reduced sensitivity to moisture attack.

Compounds 904S and 905S have cobalt which is added as an adhesion promoter. The Zn/S ratio in both these compounds is very low as compared to other steam aged compounds. Also cobalt was detected in the film in both the cases. Table VII compares the percentage of silicon in the different compounds. This shows that 904S and 905S have higher silicon content in the film. It is known that silica in the compound improves aged adhesion. Presence of cobalt reduces the conductivity of the ZnO layer and hence the sensitivity to dezincification is also reduced. Compound 905S

has a higher Cu/S ratio and Zn/S ratio. This could probably explain the lower adhesion strength in 905S as compared to 904S.

5.0 SUMMARY AND CONCLUSIONS

In this chapter the results will be summarized and then these will be compared with the results and models described in the literature. More attention will be given to the degradation of the adhesion in aging conditions. Corrosion principles as described in the model will be used to explain the results.

A technique was developed to get access to the sulfide film. Only acidified potassium per sulfate could dissolve the brass and leave the sulfide film unaffected. After getting access to the interfacial film, SEM and EDX analysis were carried out to study the effect of compound formulation.

In the unaged samples the effect of sulfur-to-accelerator level and the type of accelerator used is very apparent. Higher S/Accelerator ratios gave good sulfide films (i.e. low Cu/S ratio) and hence good adhesion strength. The accelerator DCBS was found to be better than OBTS. The type of accelerator used was more important than the sulfur to accelerator ratio, as can be seen from the comparison of compounds 899 and 903. The resin system gives very good unaged adhesion strength. The zinc content was low in all the unaged samples, which was one of the reasons for good adhesion strength.

An important criteria for good adhesion is the formation of a good sulfide film. A good sulfide film is the one which doesnot allow easy passage to diffusing

and adhesion degrading zinc ions formed by an anodic corrosion reaction underneath the ZnO layer. It is believed to consist of fine crystallites and as a result of lower copper content have lower lattice spacings, which is very compatible to the substrate lattice, hence adhere best.

The increase in adhesion strength after humidity aging could be because of the recrystallization of the sulfide film. An increase in the Cu/S ratio is seen which could mean that there has been a further growth of the film by the diffusion of copper ions. If a study of the film thickness is made then the mechanism could be understood more clearly.

The reported value of S/Cu ratio which gives the best possible adhesion is 1.8, i.e $Cu_{1.8}S$ (6). Cu/S ratio that is being studied here has sulfur from the rubber and zinc sulfide too, therefore it cannot be compared with the values given in the literature. Also difference in the film thickness could be one reason for the sometimes inconsistent trends in Cu/S ratio. After humidity aging the Cu/S increases in some compounds and decreases in some, though the strength increases in all the compounds. Growth and recrystallization are the probable mechanisms involved in humidity aging. A study of humidity aging for different times could be helpful in evaluating the quality of the interfacial film and give a better understanding of the mechanism.

Steam aging leads to the degradation of the film. Corrosion principles have been used in the literature review to explain the mechanism of degradation. An increase in the zinc content and Zn/S ratio was observed after steam aging. This is due to the diffusion of the zinc ions which was the result of an anodic corrosion reaction product. The formation of zinc hydroxide at the metal film boundary is the final cause of the

adhesion failure. The conductivities of copper sulfide and ZnO is important in preventing diffusion of the zinc ions.

In compounds 904S and 905S the presence of cobalt reduces the conductivity of ZnO (as it is incorporated as Cobalt ions) and therefore reduces the diffusion of zinc ions. The difference in adhesion strengths of 904S and 905S is due to the higher Zn/S and Cu/S ratios in 905S. The high steam aged bonding strength of 900S is difficult to explain as its film has high Zn content and high Zn/S ratio.

The mechanism of attack of steam seems to be as follows. The steam first attacks the edge of the sample and forms large amounts of zinc hydroxide at the edge interface. This reaction slowly proceeds towards the center. In the mean time due to the exposure of the edge to steam for a longer time a different set of reactions start taking place. First there is dissolution of zinc hydroxide and then due to dezincification of brass, there is a large concentration of copper on the brass surface. The copper then diffuses to the surface and forms oxides and sulfides. This explains the higher concentration of copper and lower concentration of zinc in the edge of the sample.

In compound 905S the edge has a higher zinc concentration as compared to the center. Due to the presence of cobalt the diffusion of zinc ions is retarded but it is never totally stopped. As the edge of the sample is exposed to steam for a longer duration of time the zinc ions manage to reach the interface. Also probably the copper sulfide film in 905S is a poor film, so the diffusion of zinc ions is faster than in 904S.

Figure 18 compares the compounds 899 and 904, in all conditions. This shows the effect of cobalt on adhesion strength. The trends clearly show that though cobalt does not improve the unaged adhesion much but the steam aged adhesion is

improved. However it is not able to totally prevent the decrease in adhesion after aging.

The major conclusions of this study are:-

1. Dissolution of brass by acidified Potassium per sulfate is a good technique.
2. The quality of sulfide film is most important for adhesion
3. Higher S/Accelerator ratios give better sulfide films.
4. DCBS is a better accelerator than OBTS.
5. The mechanisms of humidity aging and steam aging are different.
6. High zinc content in the interface is the cause of adhesion failure in steam aging.
7. Cobalt salts give better aged adhesion.

6.0 RECOMMENDATIONS FOR FUTURE WORK

A lot of work still has to be done before a rubber compound formulation can be optimized for the best possible adhesion in all conditions. The following areas need to be further explored in order to realize the above objective:

1. It is important to characterize the sulfide film by looking at its microstructure using TEM. Though an attempt had been made to prepare samples for TEM examination, it was not successful. A possible modification in the sample preparation may make it possible to see the microstructure, is given below.

The cause of the failure of the extraction replica technique was the strong bond between rubber and the sulfide film. Breaking the sample in liquid nitrogen leads to failure near the interface and the film goes with the brass plate. The film can be extracted from the brass plate using the replica technique. A thick piece of cellulose acetate can be used as the adhesive, which should be softened with acetone and then the brass plate should be firmly attached to it with the sulfide film facing the adhesive. After drying it and letting it bond for 24 hours the adhesive can be removed using mechanical force. The film which is now on

the adhesive can be coated with carbon. Finally, the adhesive should be totally dissolved in acetone and the film collected for TEM examination.

2. Diffraction patterns can be obtained from the TEM samples. This is useful in estimating the type of copper sulfide film formed (i.e. $Cu_{1.8}S$ or Cu_2S etc.). Then a correlation can be made with the compound formulation and the adhesion strength.
3. One of the problems encountered during this investigation was in relation to the type of microscope used. Philips 420 is an excellent microscope to do high resolution work but due to the small sample holder and the inability to go to magnifications lower than 100X the sample had to be cut into pieces. This still didnot solve the problem of seeing the whole sample at low magnification.
4. In steam aged samples, it was seen that the extreme edge of the sample had high zinc content like the center region. Hence analysis should be done along the whole diameter at many different points. This may probably indicate bands of different sulfide compositions.
5. A statistical approach is extremely important to obtain valuable information for this type of problem. Therefore analysis of many samples for one type of compound is recommended.
6. Only seven different compound formulations were studied and that too in a very qualitative manner. More new compound formulations with different S/ Accelerator ratio, adhesion promoter etc. should be studied. Study of aging samples with

different aging times may be helpful in giving an insight about the reaction mechanisms involved during aging.

7. Another possible development is the use of different alloys like CuZnNi or CuZnCo as coating materials for steel cords.

Bibliography

1. W.J. van Ooij, Rubber Chem. Technol. 52, 605 (1979).
2. W.J. van Ooij, Rubber Chem. Technol. 57, 421 (1984).
3. G.Haemers, Rubber World, Sept., 26 (1980).
4. W.J. van Ooij and M.E.F. Biemond, Rubber Chem. Technol. 51, 86 (1978).
5. J.R. Dunn, Rubber Chem. Technol. 51, 86 (1978).
6. H.Lievens, Internationale Kautschuk Tagung, June (1985).
7. W.Coppens, Plast. Rubber Proc. Appl. 2, 331 (1982).
8. W.J.van Ooij et.al., Corrosion 85, Paper 388, (1985).
9. EDX Analysis, Kevex company.

TABLE I. COMPOUND FORMULATIONS OF ALL
THE SAMPLES STUDIED

SAMPLE NUMBER	COMPOUND FORMULATION
899	BASE COMPOUND "C"
900	COMPOUND "C" WITHOUT THE RESIN SYSTEM
901	COMPOUND "C" WITH SULFUR = 4phr DCBS = 1phr
902	COMPOUND "C" WITH OBTS IN PLACE OF DCBS AT 1.25phr
903	COMPOUND "C" WITH OBTS IN PLACE OF DCBS, S/OBTS = 4
904	COMPOUND "C" WITH MONOBOND 680C = 0.5phr
905	COMPOUND 904 WITH SULFUR = 4phr ACCELERATOR = 1phr

NOTE: DCBS AND OBTS ARE ACCELERATORS
AND MONOBOND 680C IS A SALT
OF COBALT WHICH IS ADDED AS
AN ADHESION PROMOTER.

TABLE II. TABULATION OF THE ADHESION STRENGTHS OF THE SAMPLES

SAMPLE NUMBER	STRENGTH		
	UNAGED	HUMIDITY	STEAM
899	178	72	12
900	142	96	103
901	164	194	10
902	127S	155	13
903	137	156	13
904	184	186	120
905	171	181	70

TABLE III. SUMMARY OF THE SAMPLE PREPARATION TECHNIQUES.

METHOD USED	RESULT
LIQUID NITROGEN	NO SUCCESS
DIL. NITRIC ACID	PARTIAL SUCCESS
IODINE + METHANOL	NO SUCCESS
POTASSIUM PER SULFATE	SUCCESS

TABLE IV. SULFIDE FILM COMPOSITION OF ALL THE COMPOUNDS (10KV)

SAMPLE NO.	STRENGTH	AREA ANALYSED	Cu %	Zn %	S %	Cu/S	Zn/S
899H	72	CENTER	58.68	9.46	30.60	1.92	0.31
899H	72	EDGE	59.13	11.41	28.69	2.06	0.39
899S	12	CENTER	15.86	63.93	19.93	0.79	3.20
899S	12	EDGE	35.84	41.01	22.79	1.57	1.80
900S	103	CENTER	23.57	55.75	20.18	1.17	2.76
900S	103	EDGE	20.59	57.40	21.57	0.95	2.66
902S	13	CENTER	21.72	59.02	18.80	1.15	3.14
904H	186	CENTER	36.43	32.72	29.08	1.25	1.13
904S	120	CENTER	62.32	10.64	25.81	2.41	0.42
905S	70	CENTER	62.40	10.81	25.99	2.40	0.41

TABLE V. SULFIDE FILM COMPOSITION OF ALL THE COMPOUNDS (20KV)

SAMPLE NO.	STRENGTH	AREA ANALYSED	Cu %	Zn %	S %	Cu/S	Zn/S
899	178	CENTER	36.16	9.44	54.40	0.66	0.17
899H	72	CENTER	3.81	12.38	48.86	0.65	0.25
899H	72	EDGE	33.77	10.22	49.22	0.68	0.21
899S	12	CENTER	25.45	29.76	41.01	0.62	0.73
899S	12	EDGE	31.20	17.50	46.21	0.68	0.38
900S	103	CENTER	33.67	25.25	38.38	0.88	0.66
900S	103	EDGE	50.73	9.18	40.09	1.25	0.25
901	164	CENTER	41.96	3.50	54.54	0.77	0.06
901H	194	CENTER	60.28	4.47	35.25	1.71	0.13
902	127	CENTER	52.75	4.25	43.00	0.87	0.10
902H	155	CENTER	49.04	8.87	42.09	1.01	0.21
902S	13	CENTER	35.60	23.40	41.00	0.87	0.59
903	137	CENTER	47.99	5.34	46.67	1.01	0.09
903H	156	CENTER	55.72	4.69	39.58	1.41	0.12
903S	13	CENTER	39.03	27.07	33.90	1.18	0.80
903S	13	EDGE	47.64	19.49	32.87	1.50	0.62
904	184	CENTER	39.27	10.81	49.92	0.79	0.22
904H	186	CENTER	40.00	16.18	43.82	0.91	0.37
904S	120	CENTER	32.72	12.16	47.43	0.69	0.26
905	171	CENTER	56.27	3.42	40.31	1.40	0.08
905H	181	CENTER	46.57	9.20	44.23	1.05	0.21
905S	70	CENTER	33.07	14.31	45.59	0.73	0.31
905S	70	EDGE	49.48	20.98	25.08	2.00	0.85

TABLE VI. COMPARISON OF THE FILM COMPOSITION IN THE DIFFERENT REGIONS OF THE SAMPLE (AT 20KV)

SAMPLE NO.	STRENGTH	AREA ANALYSED	Cu %	Zn %	S %	Cu/S	Zn/S
899S	12	EXTREME EDGE	39.00	26.06	34.46	1.14	0.83
		EDGE	31.20	17.50	46.21	0.68	0.38
		CENTER	25.45	29.76	41.01	0.62	0.73
900S	103	EXTREME EDGE	43.30	28.98	27.71	1.56	1.01
		EDGE	50.73	9.18	40.09	1.25	0.25
		CENTER	34.03	32.04	33.92	1.00	0.94
902S	13	EXTREME EDGE	38.28	34.42	27.29	1.30	1.20
		CENTER	35.60	23.40	41.00	0.87	0.59
903S	13	EXTREME EDGE	48.27	23.56	28.17	1.70	0.83
		EDGE	47.64	19.49	32.87	1.50	0.62
		CENTER	39.03	27.07	33.90	1.18	0.80

TABLE VII. COMPARISON OF SILICON CONTENT IN STEAM AGED COMPOUNDS

COMPOUND NUMBER	% SILICON CONTENT
899S	3.79
900S	2.70
902S	3.83
904S	7.50
905S	6.90

TABLE VIII. COMPARISON OF THE FILM COMPOSITION IN UNAGED SAMPLES WITH DIFFERENT COMPOUND FORMULATIONS

SAMPLE --> NUMBER -->	899	901	902	903	904	905
STRENGTH	178	164	127	137	184	171
Cu/S	0.66	0.77	1.23	1.01	0.79	1.40
Cu	36	42	53	48	39	56
Zn	9	3.5	4	5	11	3
S	54	54	43	47	50	40

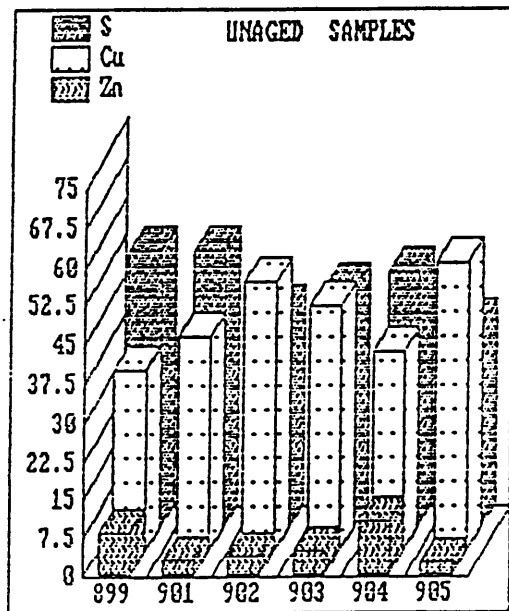


Figure 12d. Interfacial film composition of all unaged samples.

TABLE IX. COMPARISON OF THE FILM COMPOSITION IN HUMIDITY AGED SAMPLES WITH DIFFERENT COMPOUND FORMULATIONS (20KV)

SAMPLE --> NUMBER -->	899H	901H	902H	903H	904H	905H
STRENGTH	72	194	155	156	186	181
Zn/S	0.25	0.13	0.21	0.12	0.37	0.21
Cu/S	0.65	1.71	1.17	1.41	0.91	1.05
Cu %	32	60	49	56	40	46
Zn %	12	4	9	4	16	9
S %	49	35	42	39	43	44

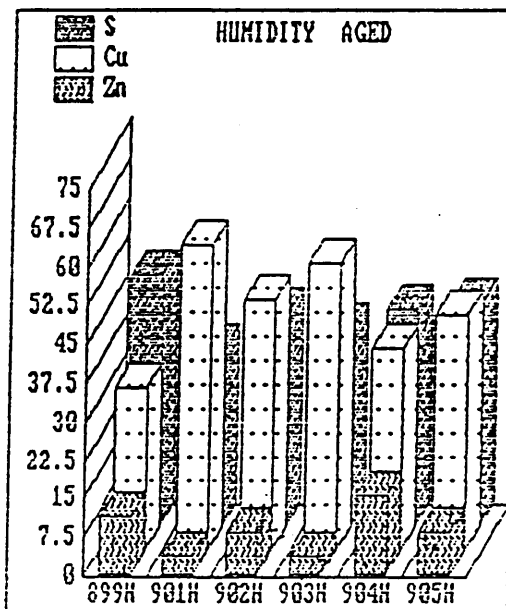


Figure 13d. Interfacial film composition of humidity aged samples

TABLE X . COMPARISON OF THE FILM COMPOSITION AT THE CENTER
 IN STEAM AGED SAMPLES WITH DIFFERENT COMPOUND
 FORMULATIONS (AT 20KV)

SAMPLE --> NUMBER -->	899S	900S	902S	903S	904S	905S
STRENGTH	12	103	13	13	120	70
Cu/S	0.62	0.88	0.83	1.18	0.69	0.72
Zn/S	0.72	0.66	0.60	0.80	0.26	0.31
Cu %	25	34	35	39	33	33
Zn %	30	25	24	27	12	14
S %	41	38	41	34	47	46

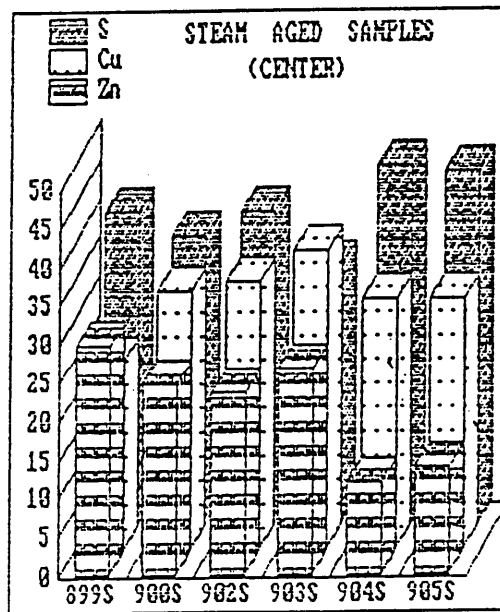


Figure 16d. Interfacial film composition of steam aged samples.

TABLE XI. COMPARISON OF THE FILM COMPOSITION AT
THE EDGE OF THE STEAM AGED SAMPLES
(AT 20KV)

SAMPLE --> NUMBER -->	899S	900S	903S	905S
STRENGTH .	12	103	13	70
Zn/S	0.38	0.25	0.62	0.85
Cu/S	0.67	1.25	1.50	2.00
Cu %	31	51	48	49
Zn %	18	9	19	21
S %	46	40	33	25

TABLE XII. COMPARISON OF THE FILM COMPOSITION
 BETWEEN HUMIDITY AND UNAGED SAMPLES
 (AT 20KV)

SAMPLE NUMBER	STRENGTH	Cu/S	Zn/S
899	178	0.66	0.17
899H	72	0.68	0.16
901	164	0.77	0.06
901H	194	1.71	0.13
902	127	1.23	0.10
902H	155	1.17	0.21
903	137	1.01	0.09
903H	156	1.41	0.12
904	184	0.79	0.22
904H	186	0.91	0.37
905	171	1.40	0.08
905H	181	1.05	0.21

TABLE XIII. COMPARISON OF THE FILM COMPOSITION
 BETWEEN STEAM AND UNAGED SAMPLES
 (AT THE CENTER AT 20KV)

SAMPLE NUMBER	STRENGTH	Cu/S	Zn/S
899	178	0.66	0.17
899S	12	0.62	0.73
902	127	1.23	0.10
902S	13	0.87	0.59
903	137	1.01	0.09
903S	13	1.18	0.80
904	184	0.79	0.22
904S	120	0.69	0.26
905	171	1.40	0.08
905S	70	0.73	0.31

TABLE XIV. COMPARISON OF THE FILM COMPOSITION
 BETWEEN STEAM AND UNAGED SAMPLES
 (AT THE EDGE AT 20KV)

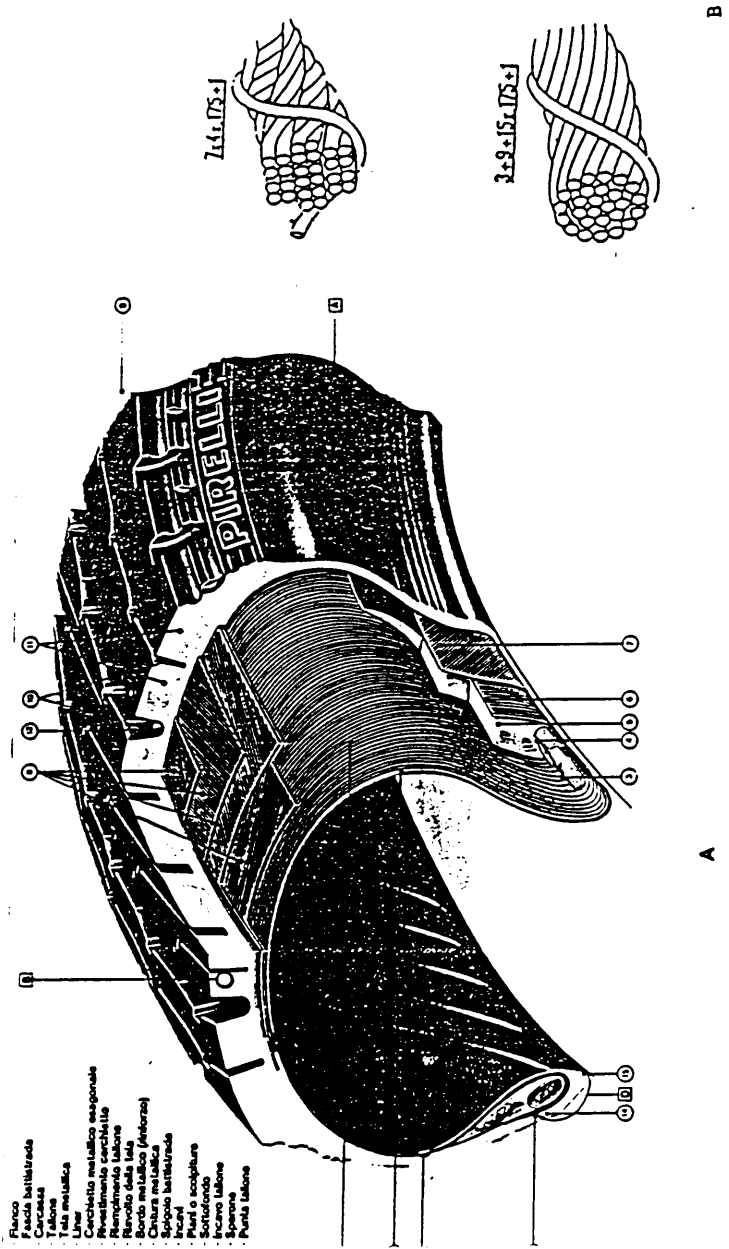
SAMPLE NUMBER	STRENGTH	Cu/S	Zn/S
899	178	0.66	0.17
899S	12	0.68	0.38
903	137	1.01	0.09
903S	13	1.50	0.62
905	171	1.40	0.08
905S	70	2.00	0.85

TABLE XV. COMPARISON OF THE FILM COMPOSITION
 AT THE EDGE AND THE CENTER OF
 THE SAMPLES (AT 20KV)

SAMPLE NUMBER	AREA ANALYSED	Cu/S	Zn/S
899S	CENTER	0.62	0.73
	EDGE	0.68	0.38
900S	CENTER	1.00	0.94
	EDGE	1.25	0.25
903S	CENTER	1.18	0.80
	EDGE	1.50	0.62
905S	CENTER	0.73	0.31
	EDGE	2.00	0.85
899H	CENTER	0.65	0.21
	EDGE	0.68	0.21

TABLE XVI. COMPARISON OF COMPOUNDS 899 AND 904
 (TO SEE THE EFFECT OF COBALT)

SAMPLE NUMBER	%	FILM COMPOSITION		
		UNAGED	HUMIDITY	STEAM
899	Cu	36.16	31.81	25.45
	Zn	9.44	12.38	29.76
	S	54.40	48.86	41.01
904	Cu	39.27	40.00	32.72
	Zn	10.81	16.18	12.16
	S	49.92	43.82	47.43

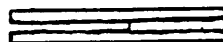


- Flanco
- Fascia battistrada
- Caricassi
- Talone
- Linea metallica
- Cerchietto metallico esponibile
- Rivestimento cerchietto
- Rivestimento talone
- Spina metallica
- Bordi metallico (anteriore)
- Cintura metallica
- Spigolo battistrada
- Puntali
- Puntali scappature
- Sottotondo
- Incarro talone
- Spessore
- Punta talone

Figure 1b. A) Nomenclature of the parts of a tubeless truck tire.
 B) Construction of brass-plated steel tire cords.



3cm



Bonding Area = 1cm X 1cm

Width of the Brass strip = 1cm

Thickness of the Rubber = 0.5mm

FIGURE 2. Dimensions of a typical sample used in this investigation.

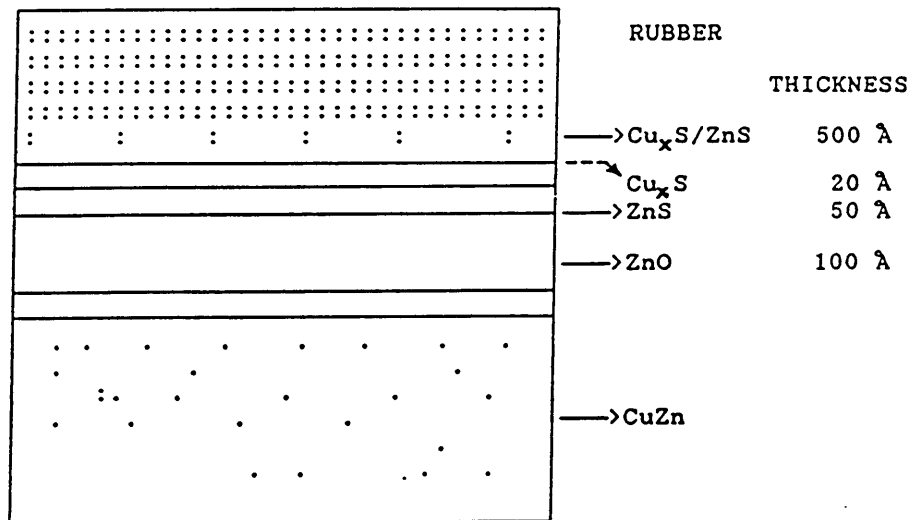


Figure 3 . Schematic of interfacial sulfide film in rubber brass bonding, showing mechanical interlocking. (Ref. 2)

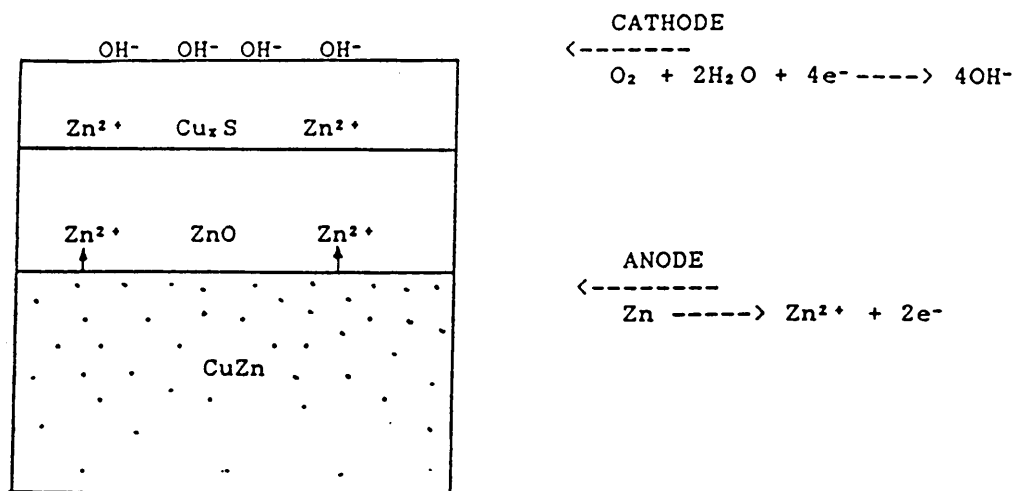
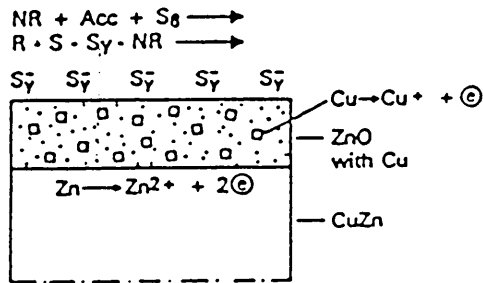
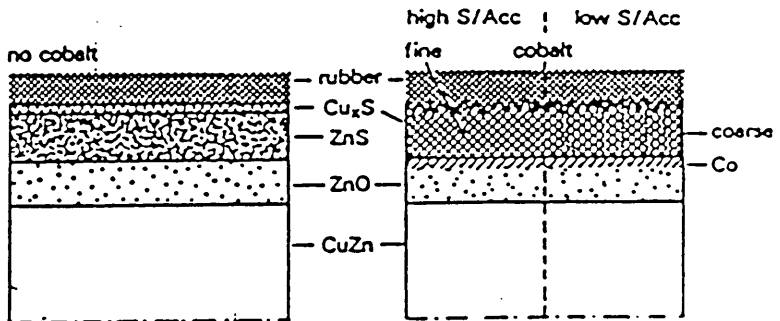


Figure 4 Schematic of effect of oxygen and H_2O on brass corrosion. (Dezincification) (Ref.2)

Before
vulcanization



Vulcanized



Aged

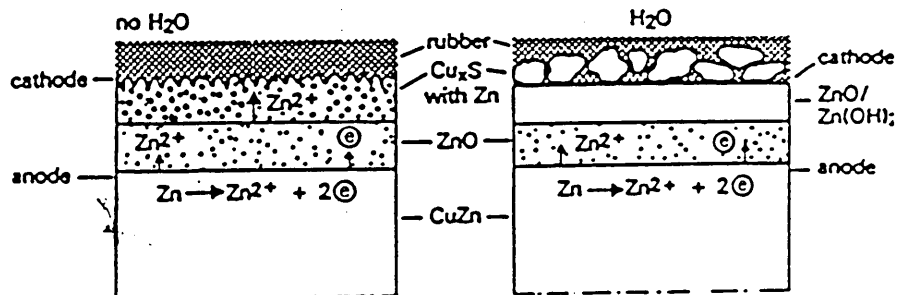


Figure 5. Schematic representation of the mechanism of rubber brass adhesion degradation during aging. (Ref. 4)

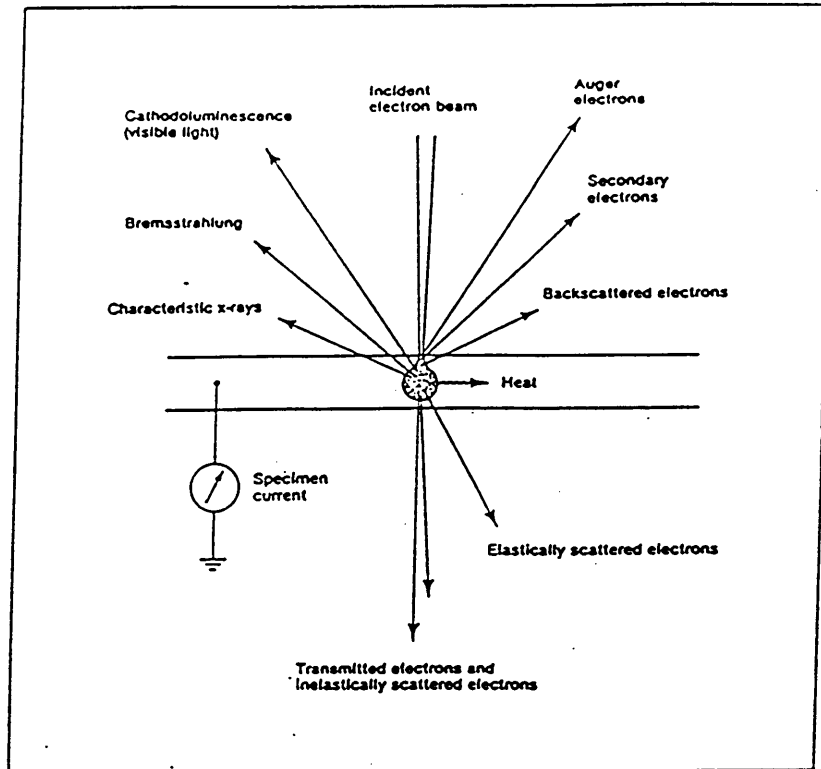


Figure 6. Schematic illustration of the principal results of the interaction of an electron beam with a specimen.

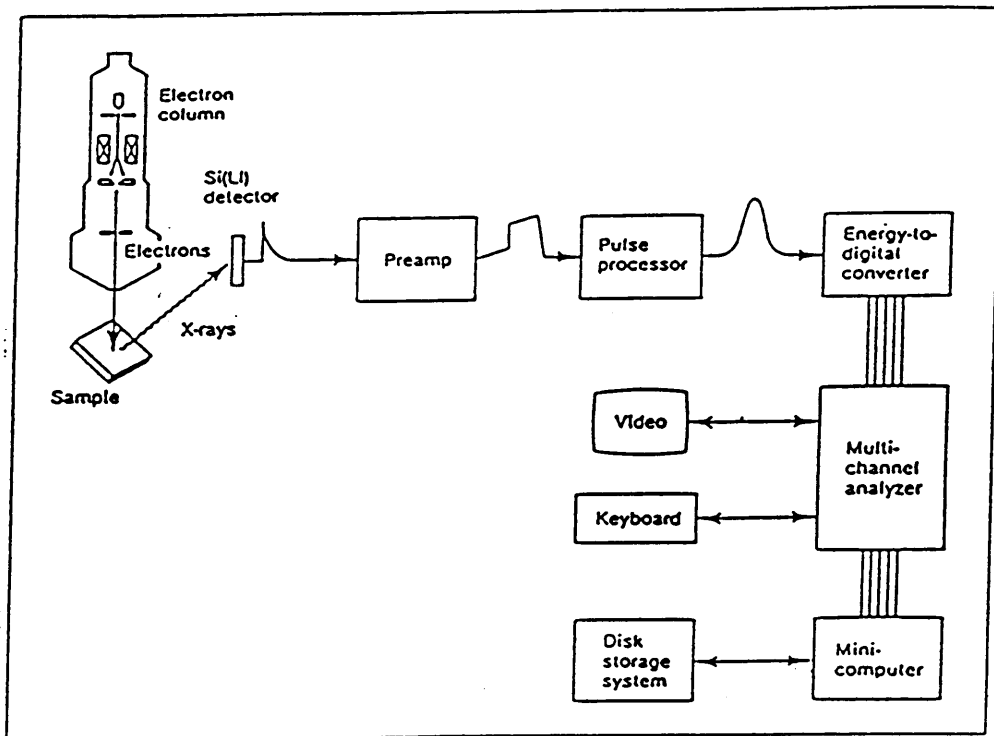


Figure 7 Components of a typical energy dispersive microanalysis system.

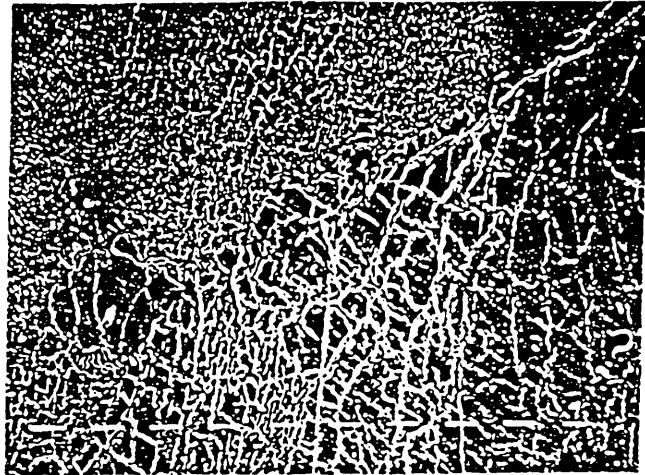


X6400 BY $K_2S_2O_8$ (902)



X6400 BY HNO_3 (901)

Figure 8 Comparison of the results of dissolution by HNO_3 acid and $K_2S_2O_8$.



X100



X3200



X800

Figure 9. Typical interfacial film in unaged samples at different magnifications (903).



X800 Cu rich region (899S)



X1600 Zn rich region (899S)



X6400 Cu rich region (900S)



X6400 Zn rich region (900S)

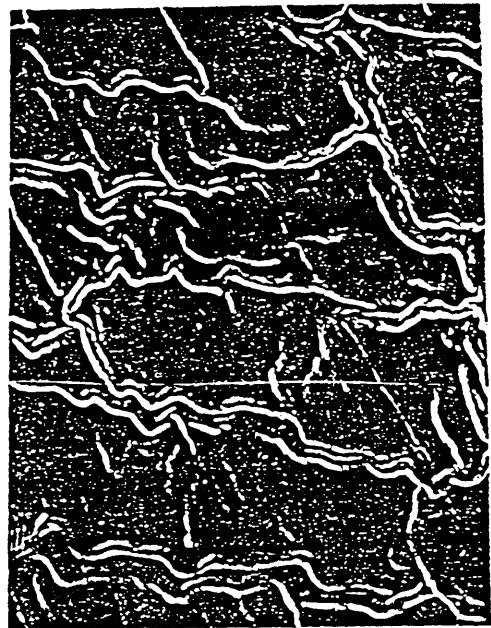
Figure 10 Comparison between zinc rich and copper rich regions in steam aged samples.



X800 UNAGED (903)



X6400 STEAM AGED (899S)



X1600 HUMIDITY AGED (903H)

Figure 11. Comparison between unaged, humidity aged and steam aged samples.

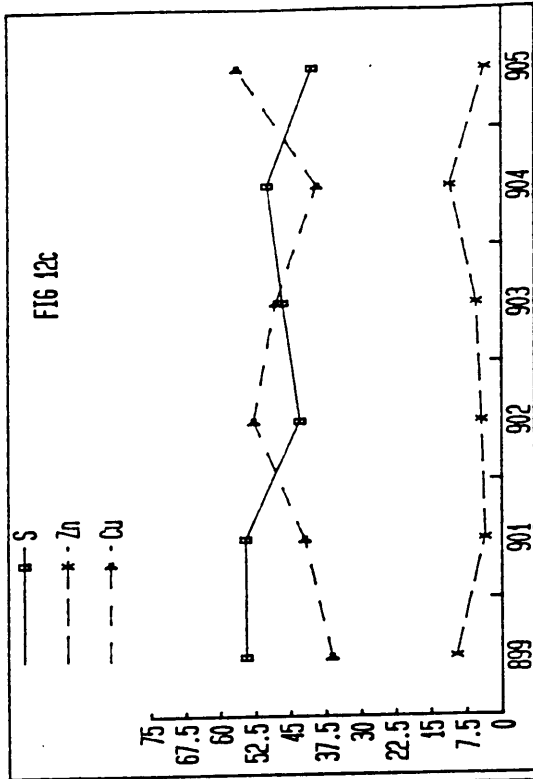
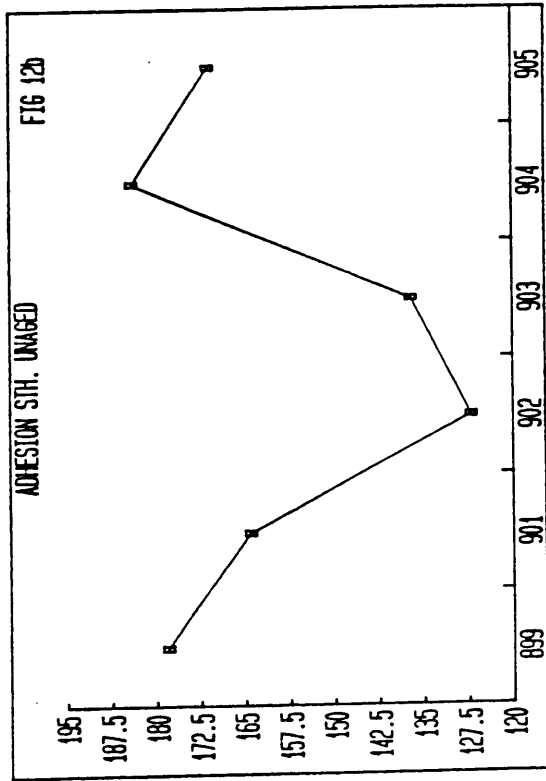
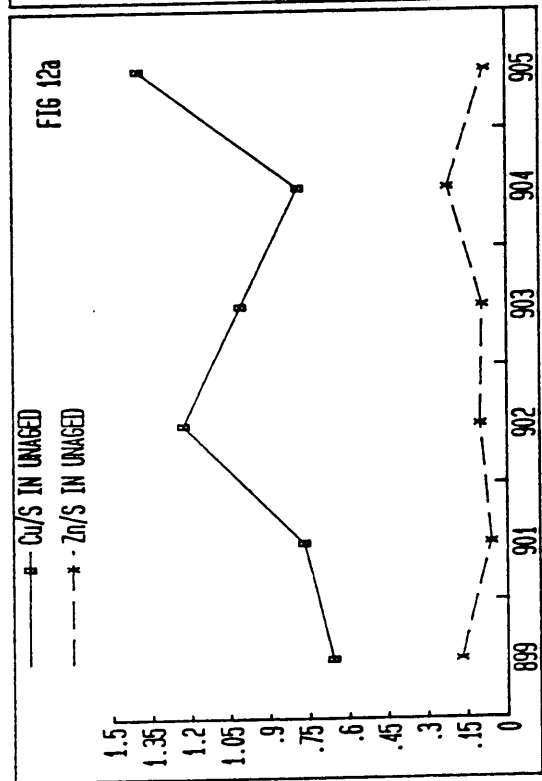


Figure 12a. Plot of Cu/S and Zn/S ratios of all unaged samples.

Figure 12b. Plot of the adhesion strengths of all unaged samples.

Figure 12c. Plot of S, Cu and Zn contents of all unaged samples.

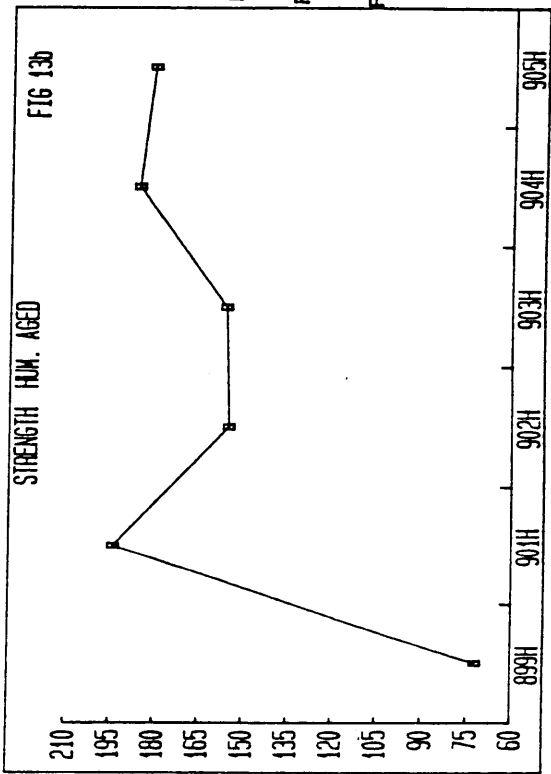
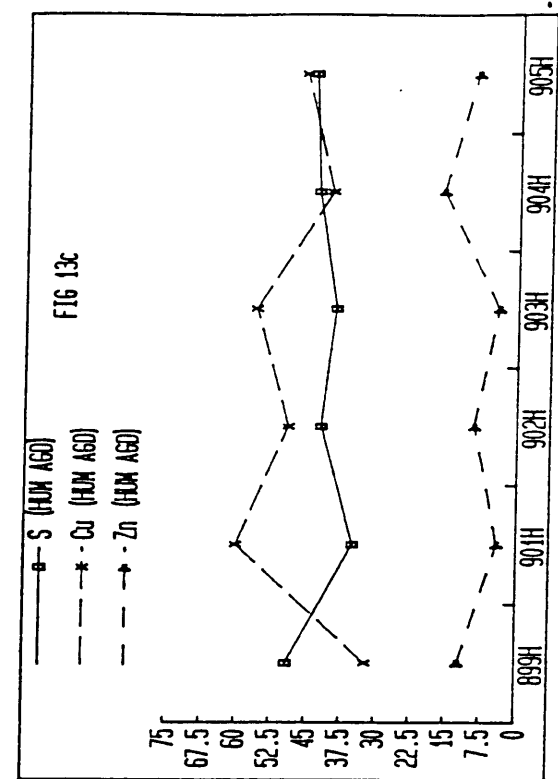
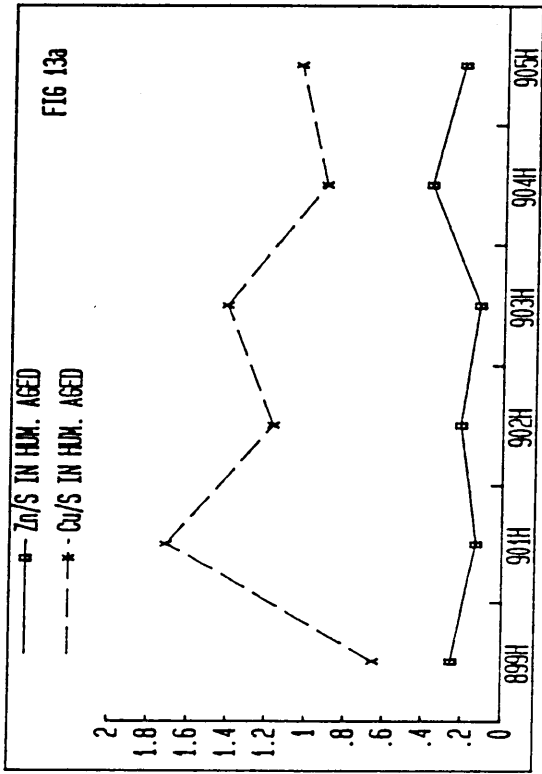


Figure 13a. Plot of Cu/S and Zn/S ratios of all humidity aged samples.

Figure 13b. Plot of adhesion strengths of all humidity aged samples.

Figure 13c. Plot of S, Cu and Zn contents of all humidity aged samples.

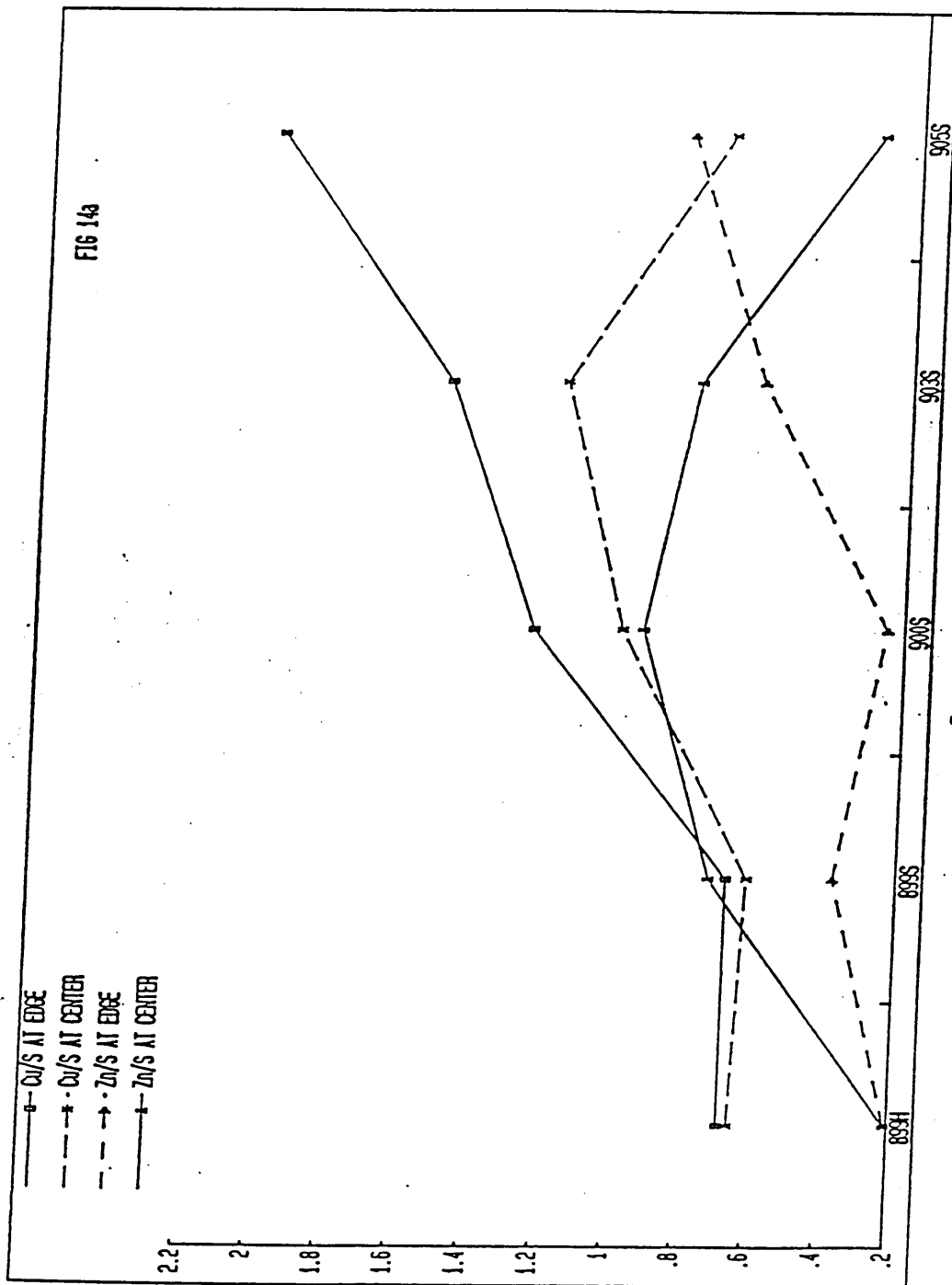


Figure 14a. Plot of Cu/S and Zn/S ratios at the center and the edge.

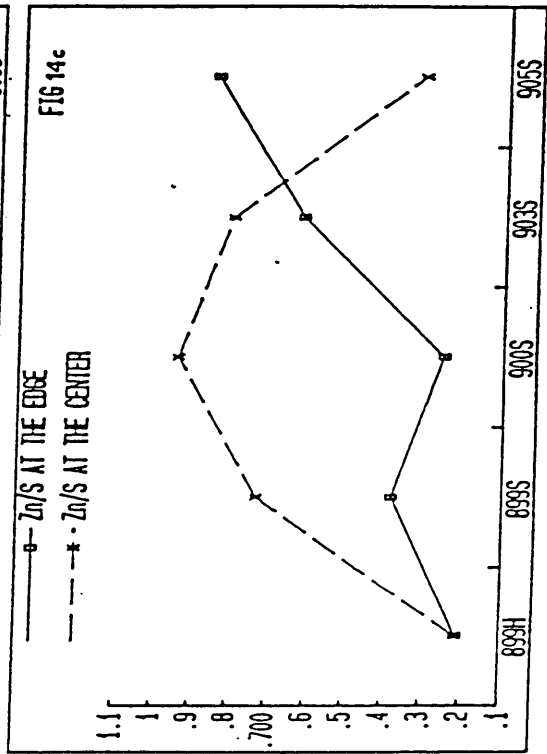
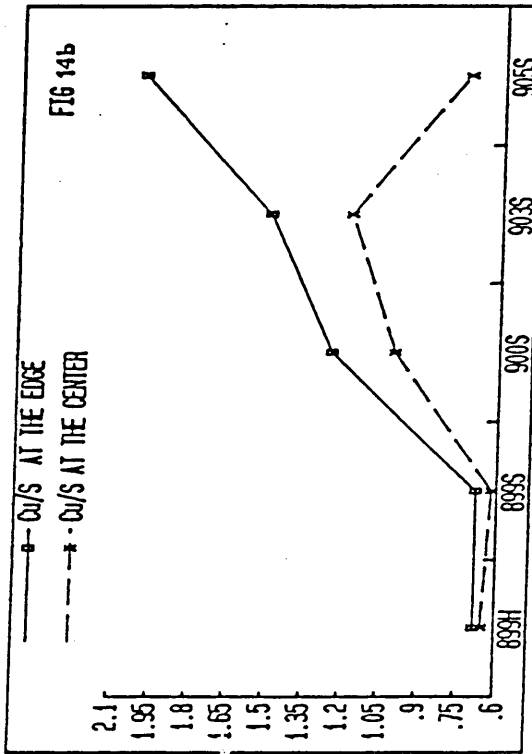


Figure 14b. Comparison of Cu/S ratio between the center and the edge.

Figure 14c. Comparison of Zn/S ratio between the center and the edge.

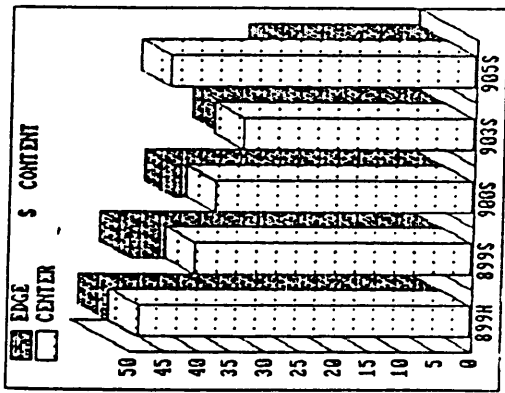


Figure 14d. Comparison of sulfur content between the center and the edge.

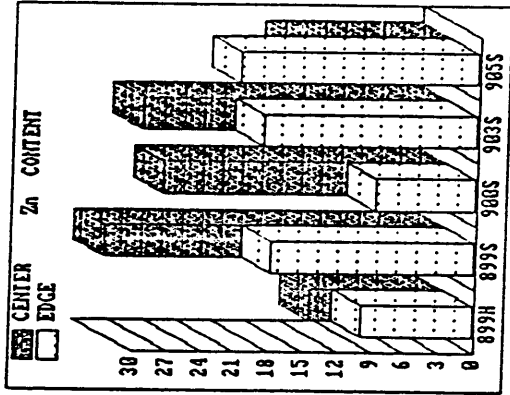


Figure 14e. Comparison of zinc content between the center and the edge.

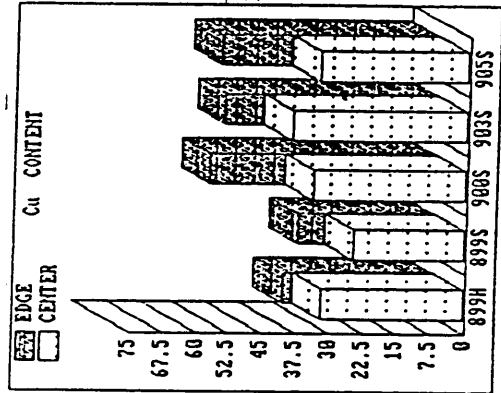


Figure 14f. Comparison of copper content between center and the edge.

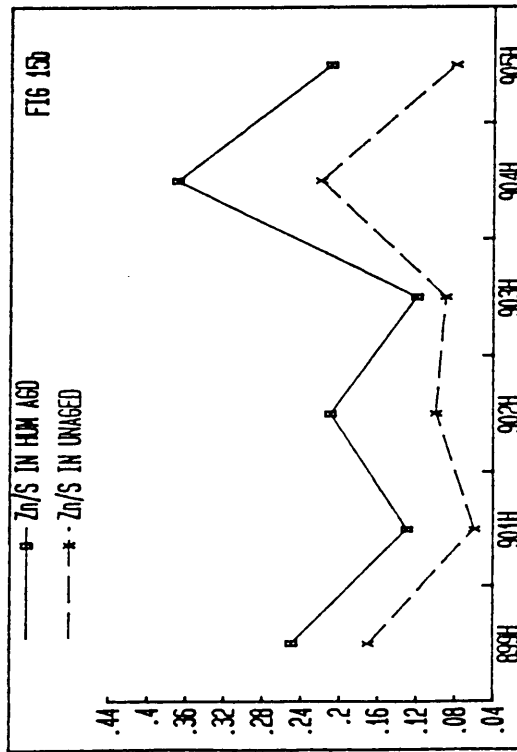
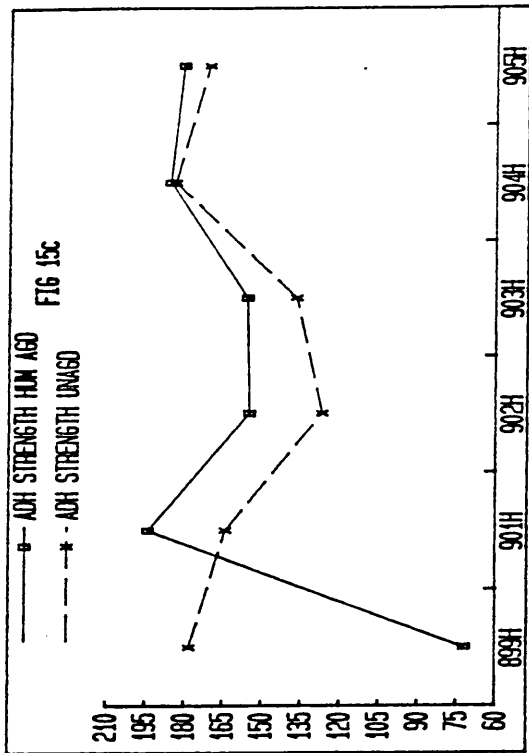
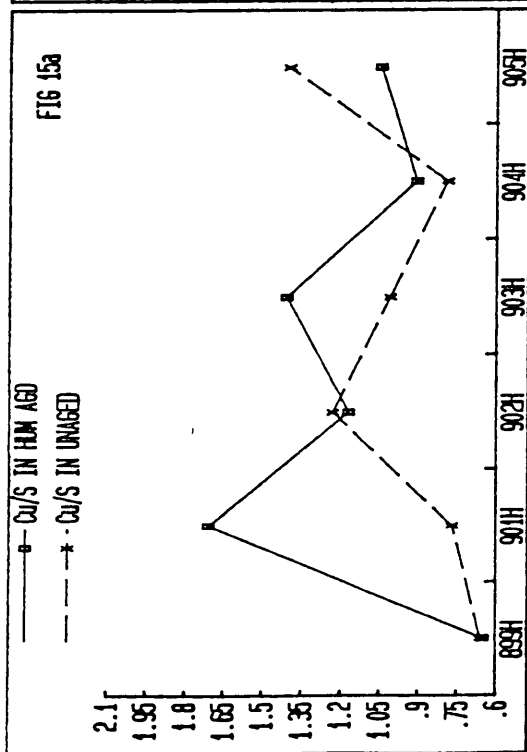


Figure 15a. Comparison of Cu/S ratio between humidity aged and unaged samples.

Figure 15b. Comparison of Zn/S ratio between humidity aged and unaged samples.

Figure 15c. Comparison of adhesion strength between humidity aged and unaged samples.

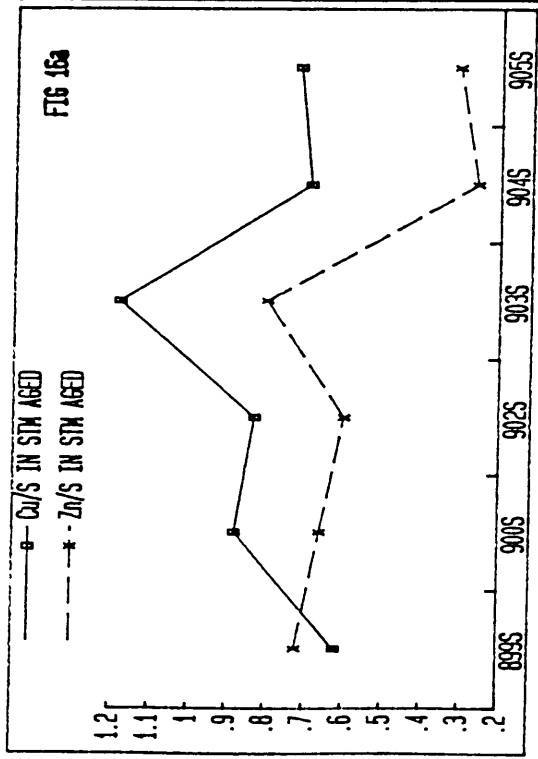


Figure 16a. Plot of Cu/S and Zn/S ratio of the steam aged samples.

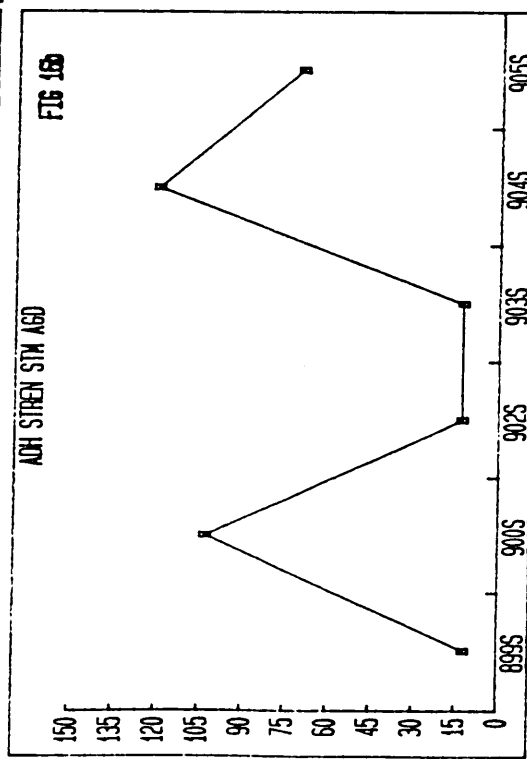


Figure 16b. Plot of adhesion strengths of all steam aged samples.

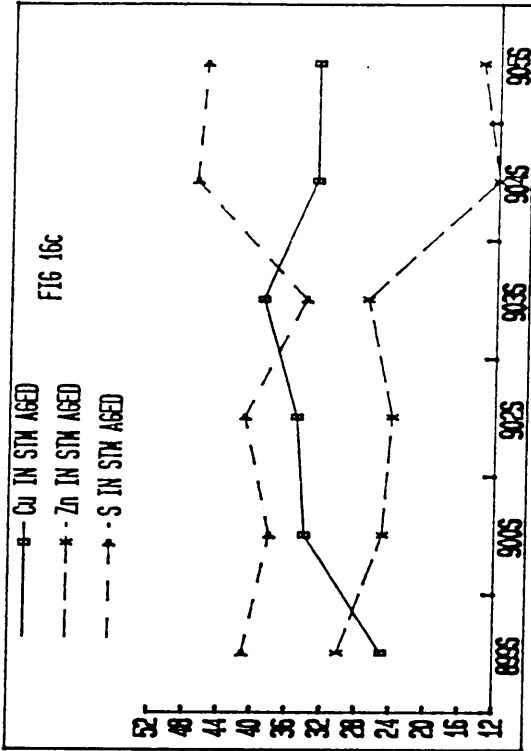


Figure 16c. Plot of S, Cu and Zn contents of steam aged samples.

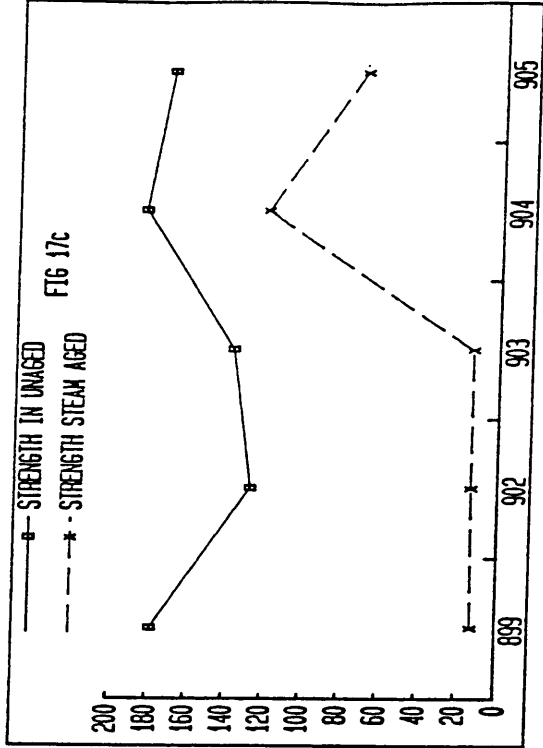
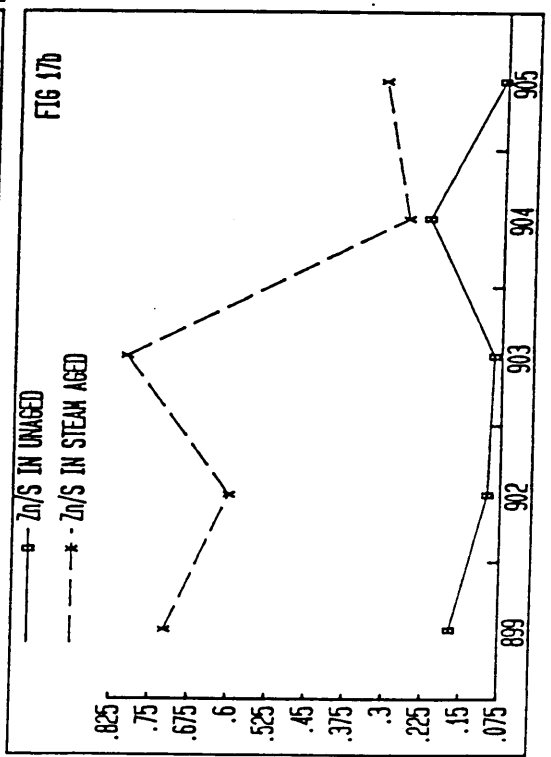
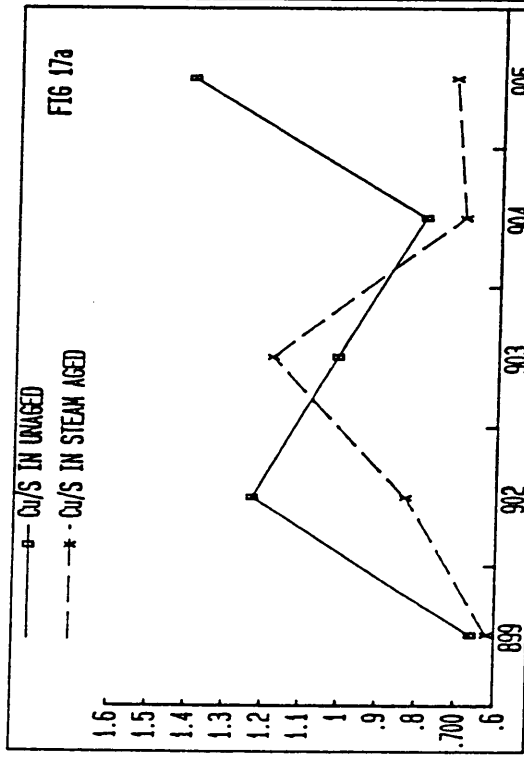


Figure 17a. Comparison of Cu/S ratio between steam aged and unaged samples.

Figure 17b. Comparison of Zn/S ratio between steam aged and unaged samples.

Figure 17c. Comparison of adhesion strengths between steam aged and unaged samples.

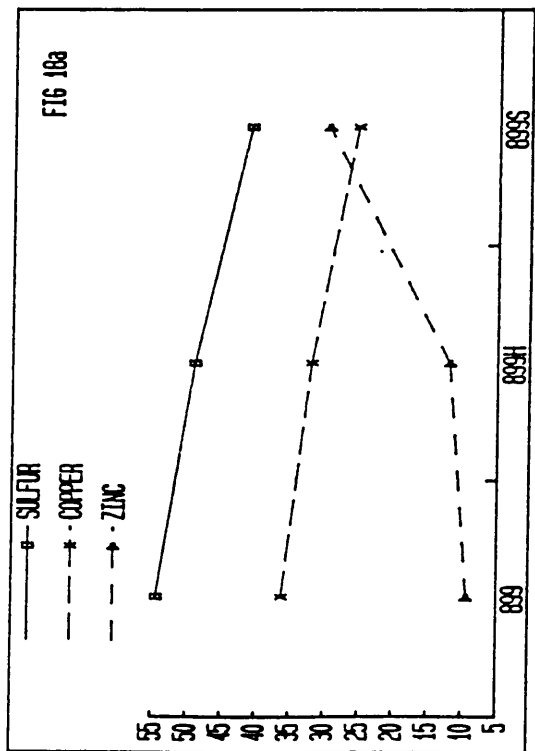


Figure 18a. Plot of S, Cu and Zn contents in compound 899 in different aging conditions.

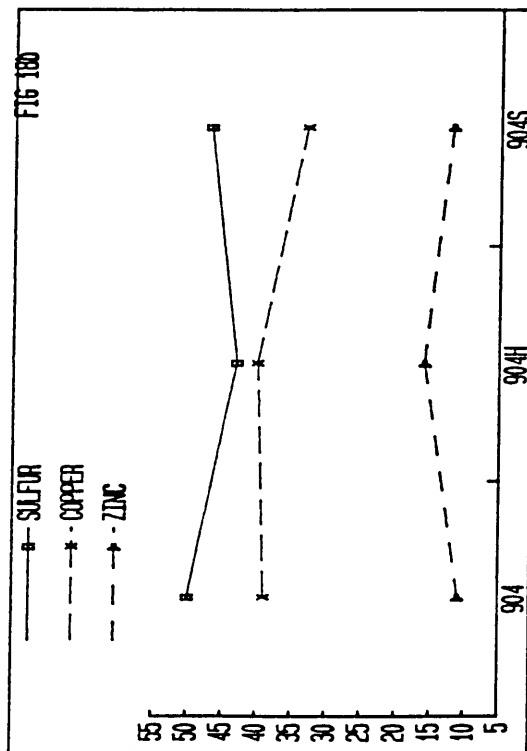


Figure 18b. Plot of S, Cu and Zn contents in compound 904 in different aging conditions.

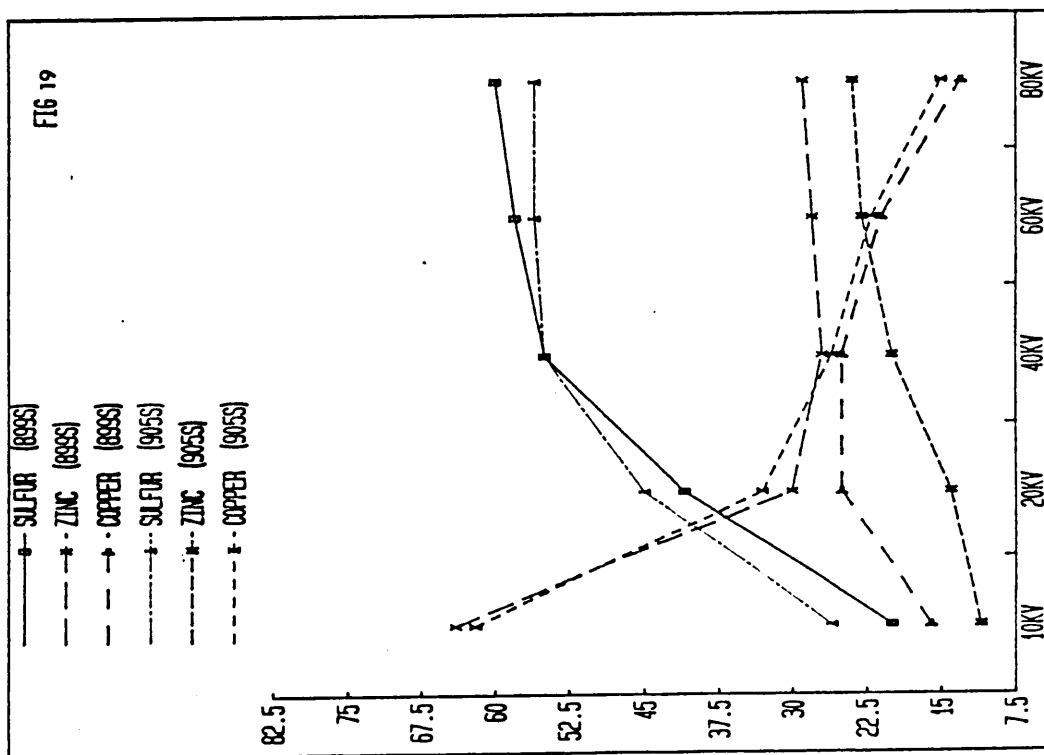


Figure 19. Comparison of depth profiles of compounds 899S and 905S.

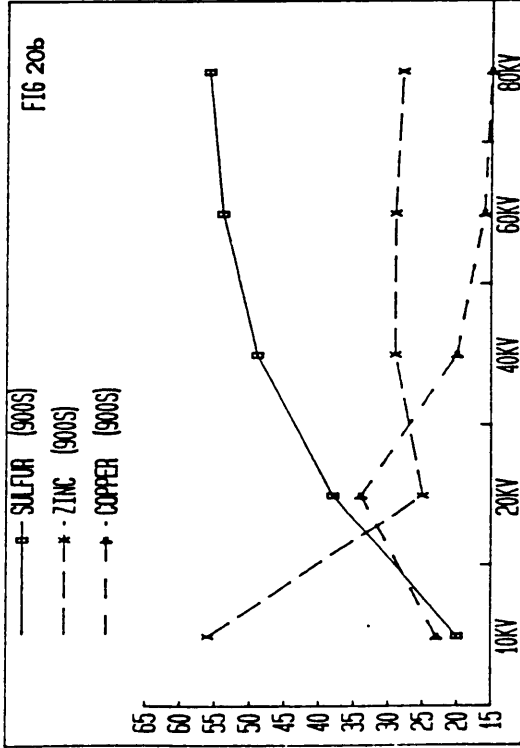
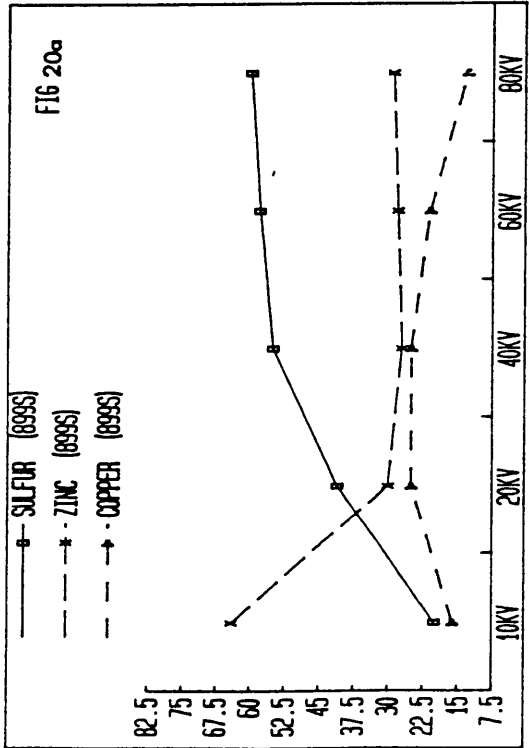
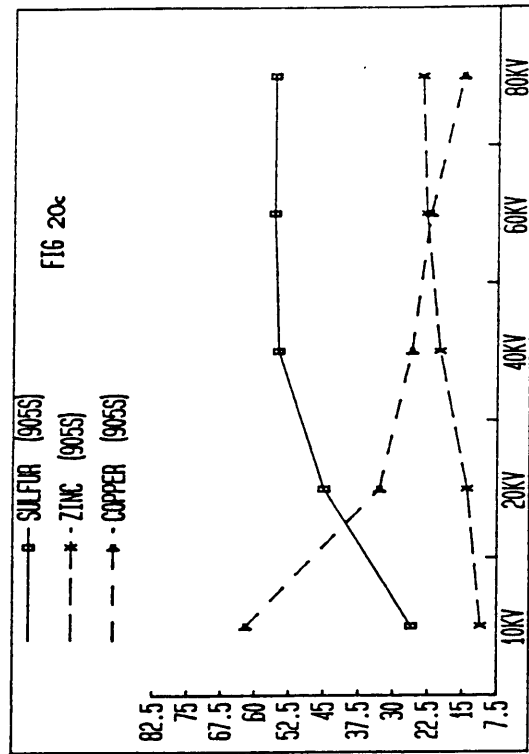


Figure 20a. Depth profile of all elements in 8995.

Figure 20b. Depth profile of all elements in 9005.

Figure 20c. Depth profile of all elements in 9055.

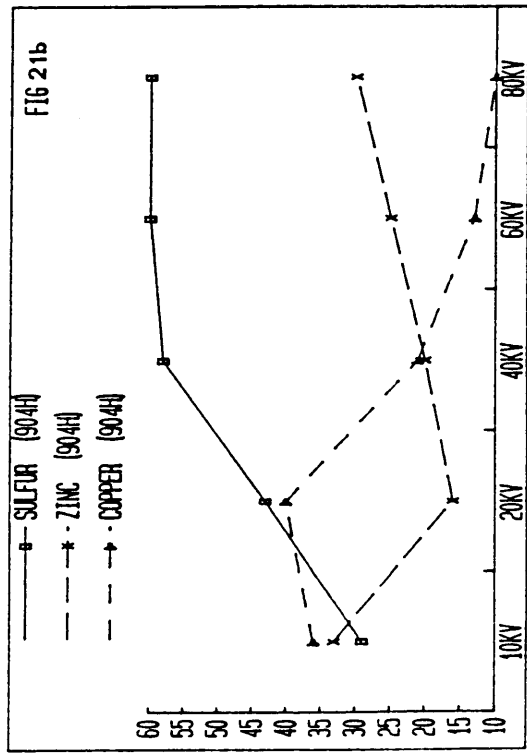
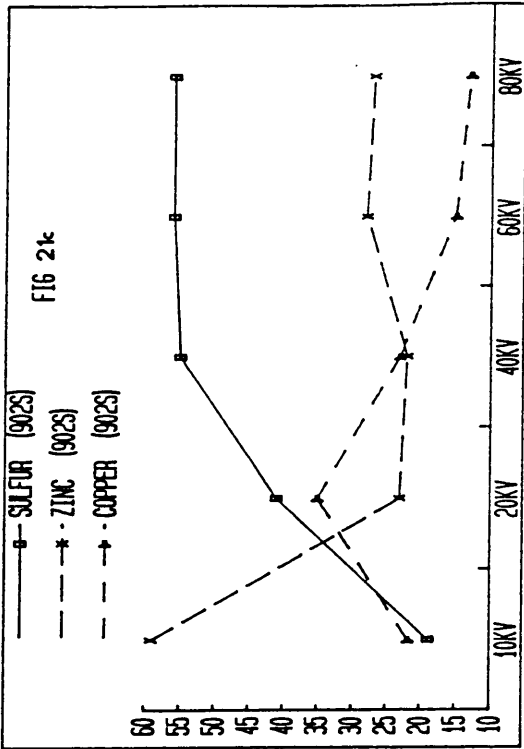
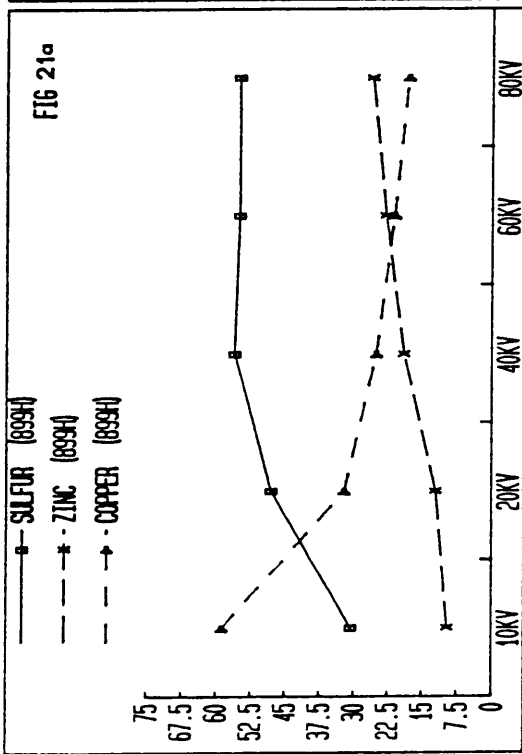


Figure 21a. Depth profile of all elements in 899H

Figure 21b. Depth profile of all elements in 904H

Figure 21c. Depth profile of all elements in 902S

TABLE VII. .COMPARISON OF SILICON CONTENT IN STEAM AGED COMPOUNDS

COMPOUND NUMBER	SILICON CONTENT %
899S	3.79
900S	2.70
902S	3.83
904S	7.50
905S	6.90

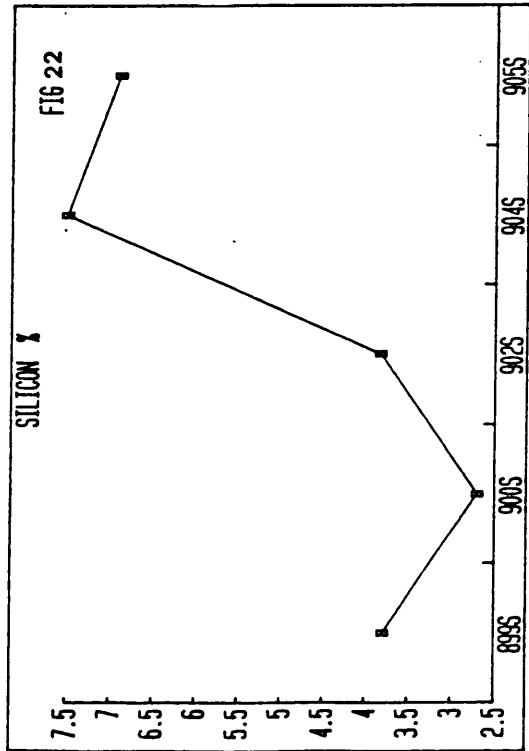


Figure 22. Plot of silicon contents in steam aged samples.

**The vita has been removed from
the scanned document**